

Analysis of linearized Galerkin-mixed FEMs for the time-dependent Ginzburg–Landau equations of superconductivity

Huadong Gao ^{*} and Weiwei Sun [†]

Abstract

A linearized backward Euler Galerkin-mixed finite element method is investigated for the time-dependent Ginzburg–Landau (TDGL) equations under the Lorentz gauge. By introducing the induced magnetic field $\boldsymbol{\sigma} = \mathbf{curl} \mathbf{A}$ as a new variable, the Galerkin-mixed FE scheme offers many advantages over conventional Lagrange type Galerkin FEMs. An optimal error estimate for the linearized Galerkin-mixed FE scheme is established unconditionally. Analysis is given under more general assumptions for the regularity of the solution of the TDGL equations, which includes the problem in two-dimensional nonconvex polygons and certain three dimensional polyhedrons, while the conventional Galerkin FEMs may not converge to a true solution in these cases. Numerical examples in both two and three dimensional spaces are presented to confirm our theoretical analysis. Numerical results show clearly the efficiency of the mixed method, particularly for problems on nonconvex domains.

Keywords: Ginzburg–Landau equation, linearized scheme, mixed finite element method, unconditional convergence, optimal error estimate, superconductivity.

1 Introduction

In this paper, we consider the time-dependent Ginzburg–Landau (TDGL) equations under the Lorentz gauge

$$\eta \frac{\partial \psi}{\partial t} - i\eta\kappa(\operatorname{div} \mathbf{A})\psi + \left(\frac{i}{\kappa}\nabla + \mathbf{A}\right)^2\psi + (|\psi|^2 - 1)\psi = 0, \quad (1.1)$$

$$\frac{\partial \mathbf{A}}{\partial t} - \nabla \operatorname{div} \mathbf{A} + \mathbf{curl} \operatorname{curl} \mathbf{A} + \frac{i}{2\kappa}(\psi^* \nabla \psi - \psi \nabla \psi^*) + |\psi|^2 \mathbf{A} = \mathbf{curl} \mathbf{H}_e, \quad (1.2)$$

for $x \in \Omega$ and $t \in (0, T]$, where the complex scalar function ψ is the order parameter and the real vector-valued function \mathbf{A} is the magnetic potential. In (1.1)-(1.2), $|\psi|^2$ denotes the density of the superconducting electron pairs. $|\psi|^2 = 1$ and $|\psi|^2 = 0$ represent the perfectly superconducting state and the normal state, respectively, while $0 < |\psi|^2 < 1$ represents a mixed state. The real vector-valued function \mathbf{H}_e is the external applied magnetic field, κ is the Ginzburg–Landau parameter and η is a dimensionless constant. In the following, we set $\eta = 1$ for the sake of

^{*}School of Mathematics and Statistics, Huazhong University of Science and Technology, Wuhan 430074, P.R. China. huadong@hust.edu.cn. The work of the author was supported in part by the National Science Foundation of China No. 11501227.

[†]Department of Mathematics, City University of Hong Kong, Kowloon, Hong Kong. maweiw@math.cityu.edu.hk. The work of the author was supported in part by a grant from the Research Grants Council of the Hong Kong Special Administrative Region, China. (Project No. CityU 11302514).

simplicity. We assume that Ω is a simply-connected bounded Lipschitz domain in \mathbb{R}^3 . The following boundary and initial conditions are supplemented to (1.1)-(1.2)

$$\frac{\partial \psi}{\partial \mathbf{n}} = 0, \quad \mathbf{curl} \mathbf{A} \times \mathbf{n} = \mathbf{H}_e \times \mathbf{n}, \quad \mathbf{A} \cdot \mathbf{n} = 0, \quad \text{on } \partial\Omega \times [0, T], \quad (1.3)$$

$$\psi(x, 0) = \psi_0(x), \quad \mathbf{A}(x, 0) = \mathbf{A}_0(x), \quad \text{in } \Omega, \quad (1.4)$$

where \mathbf{n} is the outward unit normal vector. We note that in (1.1)-(1.4), ∇ , div and \mathbf{curl} are the standard gradient, divergence and rotation operators in three dimensional space.

The TDGL equations were first deduced by Gor'kov and Eliashberg in [26] from the microscopic Bardeen–Cooper–Schrieffer theory of superconductivity. For detailed physical description and mathematical modeling of the superconductivity phenomena, we refer to the review articles [10, 20]. Theoretical analysis for the TDGL equations can be found in literature [14, 21, 29, 38, 39]. The global existence and uniqueness of the strong solution were established in [14] for the TDGL equations with the Lorentz gauge. Numerical methods for solving the TDGL equations have also been studied extensively, e.g., see [2, 13, 18, 19, 23, 27, 28, 34, 35, 37, 41]. A semi-implicit Euler scheme with a finite element approximation was first proposed by Chen and Hoffmann [13] for the TDGL equations with the Lorentz gauge. A suboptimal L^2 error estimate was obtained for the equations in two dimensional space. Later, a decoupled alternating Crank–Nicolson Galerkin method was proposed by Mu and Huang [35]. An optimal error estimate was presented under the time step restrictive conditions $\tau = O(h^{\frac{11}{12}})$ for the two-dimensional model and $\tau = O(h^2)$ for the three-dimensional model, where h and τ are the mesh size in the spatial direction and the time direction, respectively. All these schemes in [13, 18, 35] are nonlinear. At each time step, one has to solve a nonlinear system. Clearly, more commonly-used discretizations for nonlinear parabolic equations are linearized schemes, which only require the solution of a linear system at each time step. A linearized Crank–Nicolson type scheme was proposed in [34] for slightly different TDGL equations and a systematic numerical investigation was made there. An optimal error estimate of a linearized Crank–Nicolson Galerkin FE scheme for the TDGL equations was provided unconditionally in a recent work [23].

All these methods mentioned above were introduced to solve the TDGL equations (1.1)-(1.4) for the order parameter ψ and the magnetic potential \mathbf{A} by Galerkin FEMs (or finite difference methods) and then, to calculate the magnetic field $\mathbf{curl} \mathbf{A}$ by certain numerical differentiation. There are several drawbacks for such approaches. One of important issues in the study of the vortex motion in superconductors is the influence of geometric defects, which is of high interest in physics and can be considered as a problem in polygons. Previous numerical results [22, 23, 34] by conventional Lagrange FEMs showed the singularity and inaccuracy of the numerical solution around corners of polygons. Moreover, for the problem in a nonconvex polygon, conventional Lagrange FEMs for the TDGL equations may converge to a spurious solution, see the numerical experiments reported in [22, 32] for the problem on an L -shape domain. Another issue in the superconductivity model is its coupled boundary conditions in (1.3), which may bring some extra difficulties in implementation to conventional Lagrange FEMs on a general domain, see section 5 of [12] for more detailed description. It is natural that a mixed finite element method with the physical quantity $\boldsymbol{\sigma} = \mathbf{curl} \mathbf{A}$ being the new variable may offer many advantages.

It has been noted that mixed methods for second order elliptic problems, such as the scalar Poisson equation $-\Delta u = f$ with simple boundary conditions, Dirichlet or Neumann, have been well studied with the extra variable $\mathbf{v} = \nabla u$ in the last several decades, e.g., see [8, 9, 24, 25, 40] and references therein. However, mixed finite element methods for the vector Poisson equation $-\Delta \mathbf{u} = \mathbf{f}$ with the coupled boundary conditions $\mathbf{curl} \mathbf{u} \times \mathbf{n} = \mathbf{g}$ and $\mathbf{u} \cdot \mathbf{n} = 0$ seems much more complicated than for a scalar equation. Theoretical analysis was established quite recently

[4, 5] in terms of finite element exterior calculus. For the TDGL equations (2.13)-(2.16) in two dimensional space, Chen [12] proposed a semi-implicit and weakly nonlinear scheme with a mixed finite element method, in which both $\mathbf{curl} \mathbf{A}$ and $\mathbf{div} \mathbf{A}$ were introduced to be extra unknowns, and the corresponding finite element spaces for $\mathbf{curl} \mathbf{A}$ and $\mathbf{div} \mathbf{A}$ were constructed with certain bubble functions and some special treatments in elements adjacent to the boundary of the domain were also needed. A suboptimal L^2 error estimate was provided and no numerical example was given in [12]. Recently, a linearized backward Euler Galerkin-mixed finite element method was proposed in [22] for the TDGL equations in both two and three dimensional spaces with only one extra physical quantity $\boldsymbol{\sigma} = \mathbf{curl} \mathbf{A}$ ($\boldsymbol{\sigma} = \mathbf{curl} \mathbf{A}$ in two dimensional space). No analysis was provided in [22]. The scheme is decoupled and at each time step, one only needs to solve two linear systems for ψ and $(\mathbf{A}, \boldsymbol{\sigma})$, which can be done simultaneously.

This paper focuses on theoretical analysis on a linearized Galerkin-mixed FEM for the TDGL equations to establish optimal error estimates. More important is that our analysis is given without any time-step restrictions and under more general assumptions for the regularity of the solution of the TDGL equations, which includes the problem in nonconvex polygons and certain convex polyhedrons. Usually, conventional FEMs for a scalar parabolic equation require the regularity of the solution in H^{1+s} with $s > 0$ [11, 15], while for the TDGL equations in a nonconvex polygon, $\mathbf{A} \in \mathbf{H}^s$ and $\mathbf{curl} \mathbf{A}, \mathbf{div} \mathbf{A} \in H^{1+s}$ with $s < 1$ in general [31]. Our numerical results show clearly that the mixed method converges to a true solution for problems in a nonconvex polygon and conventional Lagrange type FEMs do not in this case. In addition, in the mixed FEM, the coupled boundary condition $\mathbf{curl} \mathbf{A} \times \mathbf{n} = \mathbf{H}_e \times \mathbf{n}$ reduces to a Dirichlet type boundary condition $\boldsymbol{\sigma} \times \mathbf{n} = \mathbf{H}_e \times \mathbf{n}$. Implementation of Dirichlet boundary conditions for vector-valued elements (such as Nédélec and Raviart–Thomas elements) becomes much simpler. In a recent work by Li and Zhang, an approach based on Hodge decomposition was proposed and analyzed with optimal error estimates. However, the approach is applicable only for the problem in two-dimensional space due to the restriction of the Hodge decomposition.

The rest of this paper is organized as follows. In section 2, we introduce the linearized backward Euler scheme with Galerkin-mixed finite element approximations for the TDGL equations and we present our main results on unconditionally optimal error estimates. In section 3, we recall some results for an auxiliary elliptic problem of the vector Poisson equation with the coupled boundary conditions. In section 4, we prove that an optimal L^2 error estimate holds almost unconditionally (*i.e.*, without any mesh ratio restriction). In section 5, we provide several numerical examples to confirm our theoretical analysis and show the efficiency of the proposed methods. Some concluding remarks are given in section 6.

2 A linearized backward Euler Galerkin-mixed FEM

In this section, we present a linearized backward Euler Galerkin-mixed finite element method for the TDGL equations and our main results. For simplicity, we introduce some standard notations and operators below. For any two complex functions $u, v \in \mathcal{L}^2(\Omega)$, we denote the $\mathcal{L}^2(\Omega)$ inner product and norm by

$$(u, v) = \int_{\Omega} u(x) (v(x))^* dx, \quad \|u\|_{L^2} = (u, u)^{\frac{1}{2}},$$

where v^* denotes the conjugate of the complex function v . Let $W^{k,p}(\Omega)$ be the Sobolev space defined on Ω , and by conventional notations, $H^k(\Omega) := W^{k,2}(\Omega)$, $\mathring{H}^k(\Omega) := \mathring{W}^{k,2}(\Omega)$. Let $\mathcal{H}^k(\Omega) = \{u + iv \mid u, v \in H^k(\Omega)\}$ be a complex-valued Sobolev space and $\mathbf{H}^k(\Omega) = [H^k(\Omega)]^d$

be a vector-valued Sobolev space, where d is the dimension of Ω . For a positive real number $s = k + \theta$ with $0 < \theta < 1$, we define $H^s(\Omega) = (H^k, H^{k+1})_{[\theta]}$ by the complex interpolation, see [6]. To introduce the mixed variational formulation, we denote

$$\mathbf{H}(\text{div}) = \{\mathbf{A} \mid \mathbf{A} \in \mathbf{L}^2(\Omega), \text{div } \mathbf{A} \in L^2(\Omega)\} \text{ with } \|\mathbf{A}\|_{\mathbf{H}(\text{div})} = (\|\mathbf{A}\|_{L^2}^2 + \|\text{div } \mathbf{A}\|_{L^2}^2)^{\frac{1}{2}}$$

and

$$\mathbf{H}(\text{curl}) = \{\mathbf{A} \mid \mathbf{A} \in \mathbf{L}^2(\Omega), \text{curl } \mathbf{A} \in L^2(\Omega)\} \text{ with } \|\mathbf{A}\|_{\mathbf{H}(\text{curl})} = (\|\mathbf{A}\|_{L^2}^2 + \|\text{curl } \mathbf{A}\|_{L^2}^2)^{\frac{1}{2}}.$$

Also we define

$$\mathring{\mathbf{H}}(\text{div}) = \{\mathbf{A} \mid \mathbf{A} \in \mathbf{H}(\text{div}), \mathbf{A} \cdot \mathbf{n}|_{\partial\Omega} = 0\}$$

and its dual space $\mathring{\mathbf{H}}(\text{div})'$ with norm

$$\|\mathbf{v}\|_{\mathring{\mathbf{H}}(\text{div})'} := \sup_{\mathbf{w} \in \mathring{\mathbf{H}}(\text{div})} \frac{(\mathbf{v}, \mathbf{w})}{\|\mathbf{w}\|_{\mathbf{H}(\text{div})}}.$$

Moreover, we denote

$$\mathring{\mathbf{H}}(\text{curl}) = \{\mathbf{A} \mid \mathbf{A} \in \mathbf{H}(\text{curl}), \mathbf{A} \times \mathbf{n}|_{\partial\Omega} = \mathbf{0}\}.$$

By introducing $\boldsymbol{\sigma} = \text{curl } \mathbf{A}$, the mixed form of the TDGL equations (1.1)-(1.4) can be written by

$$\frac{\partial \psi}{\partial t} - i\kappa(\text{div } \mathbf{A})\psi + \left(\frac{i}{\kappa}\nabla + \mathbf{A}\right)^2\psi + (|\psi|^2 - 1)\psi = 0, \quad (2.1)$$

$$\boldsymbol{\sigma} = \text{curl } \mathbf{A}, \quad (2.2)$$

$$\frac{\partial \mathbf{A}}{\partial t} - \nabla \text{div } \mathbf{A} + \text{curl } \boldsymbol{\sigma} + \frac{i}{2\kappa}(\psi^* \nabla \psi - \psi \nabla \psi^*) + |\psi|^2 \mathbf{A} = \text{curl } \mathbf{H}_e, \quad (2.3)$$

with boundary and initial conditions

$$\frac{\partial \psi}{\partial \mathbf{n}} = 0, \quad \boldsymbol{\sigma} \times \mathbf{n} = \mathbf{H}_e \times \mathbf{n}, \quad \mathbf{A} \cdot \mathbf{n} = 0, \quad \text{on } \partial\Omega \times [0, T], \quad (2.4)$$

$$\psi(x, 0) = \psi_0(x), \quad \boldsymbol{\sigma}(x, 0) = \text{curl } \mathbf{A}_0(x), \quad \mathbf{A}(x, 0) = \mathbf{A}_0(x), \quad \text{in } \Omega. \quad (2.5)$$

The mixed variational formulation of the TDGL equations (2.1)-(2.3) with boundary and initial conditions (2.4)-(2.5) is to find $\psi \in L^2(0, T; \mathcal{H}^1(\Omega))$ with $\frac{\partial \psi}{\partial t} \in L^2(0, T; \mathcal{H}^{-1}(\Omega))$, and $(\boldsymbol{\sigma}, \mathbf{A}) \in L^2(0, T; \mathbf{H}(\text{curl})) \times L^2(0, T; \mathring{\mathbf{H}}(\text{div}))$ with $\frac{\partial \mathbf{A}}{\partial t} \in L^2(0, T; \mathring{\mathbf{H}}(\text{div})')$, where $\boldsymbol{\sigma} \times \mathbf{n} = \mathbf{H}_e \times \mathbf{n}$ on $\partial\Omega$, such that

$$\begin{aligned} \left(\frac{\partial \psi}{\partial t}, \omega\right) - i\kappa((\text{div } \mathbf{A})\psi, \omega) + \left(\left(\frac{i}{\kappa}\nabla + \mathbf{A}\right)\psi, \left(\frac{i}{\kappa}\nabla + \mathbf{A}\right)\omega\right) \\ + (|\psi|^2 - 1)\psi, \omega = 0, \quad \forall \omega \in \mathcal{H}^1(\Omega) \end{aligned} \quad (2.6)$$

and

$$(\boldsymbol{\sigma}, \boldsymbol{\chi}) - (\text{curl } \boldsymbol{\chi}, \mathbf{A}) = 0, \quad \forall \boldsymbol{\chi} \in \mathring{\mathbf{H}}(\text{curl}), \quad (2.7)$$

$$\begin{aligned} \left(\frac{\partial \mathbf{A}}{\partial t}, \mathbf{v}\right) + (\text{curl } \boldsymbol{\sigma}, \mathbf{v}) + (\text{div } \mathbf{A}, \text{div } \mathbf{v}) + \frac{i}{2\kappa}((\psi^* \nabla \psi - \psi \nabla \psi^*), \mathbf{v}) \\ + (|\psi|^2 \mathbf{A}, \mathbf{v}) = (\text{curl } \mathbf{H}_e, \mathbf{v}), \quad \forall \mathbf{v} \in \mathring{\mathbf{H}}(\text{div}), \end{aligned} \quad (2.8)$$

for a.e. $t \in (0, T]$ with $\psi(x, 0) = \psi_0(x)$, $\boldsymbol{\sigma}(x, 0) = \mathbf{curl} \mathbf{A}_0(x)$ and $\mathbf{A}(x, 0) = \mathbf{A}_0(x)$.

For simplicity, we assume that Ω is a polyhedron in three dimensional space. Let \mathcal{T}_h be a quasi-uniform tetrahedral partition of Ω with $\Omega = \cup_K \Omega_K$ and denote by $h = \max_{\Omega_K \in \mathcal{T}_h} \{\text{diam } \Omega_K\}$ the mesh size. For a given partition \mathcal{T}_h , we denote by \mathcal{V}_h^r the r -th order Lagrange finite element subspace of $\mathcal{H}^1(\Omega)$. we denote by \mathbf{Q}_h^r the r -th order first type Nédélec finite element subspace of $\mathbf{H}(\mathbf{curl})$, where the case $r = 1$ corresponds to the lowest order Nédélec edge element (6 dofs). We denote by \mathbf{U}_h^r the r -th order Raviart–Thomas finite element subspace of $\mathbf{H}(\text{div})$, where the case $r = 0$ corresponds to the lowest order Raviart–Thomas face element (4 dofs). We also define $\mathring{\mathbf{Q}}_h^r = \mathbf{Q}_h^r \cap \mathring{\mathbf{H}}(\mathbf{curl})$ and $\mathring{\mathbf{U}}_h^r = \mathbf{U}_h^r \cap \mathring{\mathbf{H}}(\text{div})$. It should be remarked that Brezzi–Douglas–Marini element can also be used for approximation of $\mathbf{H}(\text{div})$. Here we only confine our attention to the Raviart–Thomas element approximation. By noting the approximation properties of the finite element spaces \mathcal{V}_h^r , \mathbf{Q}_h^r and \mathbf{U}_h^r [1, 8, 24], we denote by π_h a general projection operator on \mathcal{V}_h^r , \mathbf{Q}_h^r and \mathbf{U}_h^r , satisfying

$$\begin{cases} \|\omega - \pi_h \omega\|_{L^2} \leq Ch^s \|\omega\|_{H^s}, & 0 < s \leq r + 1, \\ \|\boldsymbol{\chi} - \pi_h \boldsymbol{\chi}\|_{L^2} + \|\mathbf{curl}(\boldsymbol{\chi} - \pi_h \boldsymbol{\chi})\|_{L^2} \leq Ch^s (\|\boldsymbol{\chi}\|_{H^s} + \|\mathbf{curl} \boldsymbol{\chi}\|_{H^s}), & \frac{1}{2} < s \leq r, \\ \|\mathbf{v} - \pi_h \mathbf{v}\|_{L^2} + \|\text{div}(\mathbf{v} - \pi_h \mathbf{v})\|_{L^2} \leq Ch^s (\|\mathbf{v}\|_{H^s} + \|\text{div} \mathbf{v}\|_{H^s}), & 0 < s \leq r + 1. \end{cases} \quad (2.9)$$

Let $\{t_n\}_{n=0}^N$ be a uniform partition in the time direction with the step size $\tau = \frac{T}{N}$, and let $u^n = u(\cdot, n\tau)$. For a sequence of functions $\{U^n\}_{n=0}^N$ defined on Ω , we denote

$$D_\tau U^n = \frac{U^n - U^{n-1}}{\tau}, \quad \text{for } n = 1, 2, \dots, N.$$

With the above notations, the linearized backward Euler Galerkin-mixed FEM for the mixed form TDGL equations (2.1)-(2.5) is to find $\psi_h^n \in \mathcal{V}_h^{\widehat{r}}$ and $(\boldsymbol{\sigma}_h^n, \mathbf{A}_h^n) \in \mathbf{Q}_h^{r+1} \times \mathring{\mathbf{U}}_h^r$, with $\boldsymbol{\sigma}_h^n \times \mathbf{n} = \pi_h \mathbf{H}_e^n \times \mathbf{n}$ on $\partial\Omega$, such that for $n = 1, 2, \dots, N$,

$$\begin{aligned} (D_\tau \psi_h^n, \omega_h) - i\kappa((\text{div} \mathbf{A}_h^{n-1})\psi_h^n, \omega_h) + ((\frac{i}{\kappa} \nabla + \mathbf{A}_h^{n-1})\psi_h^n, (\frac{i}{\kappa} \nabla + \mathbf{A}_h^{n-1})\omega_h) \\ + (|\psi_h^{n-1}|^2 - 1)\psi_h^n, \omega_h) = 0, \quad \forall \omega_h \in \mathcal{V}_h^{\widehat{r}}, \end{aligned} \quad (2.10)$$

and

$$(\boldsymbol{\sigma}_h^n, \boldsymbol{\chi}_h) - (\mathbf{curl} \boldsymbol{\chi}_h, \mathbf{A}_h^n) = 0, \quad \forall \boldsymbol{\chi}_h \in \mathring{\mathbf{Q}}_h^{r+1}, \quad (2.11)$$

$$\begin{aligned} (D_\tau \mathbf{A}_h^n, \mathbf{v}_h) + (\text{div} \mathbf{A}_h^n, \text{div} \mathbf{v}_h) + (\mathbf{curl} \boldsymbol{\sigma}_h^n, \mathbf{v}_h) + (|\psi_h^{n-1}|^2 \mathbf{A}_h^n, \mathbf{v}_h) \\ = (\mathbf{curl} \mathbf{H}_e^n, \mathbf{v}_h) - \frac{i}{2\kappa} ((\psi_h^{n-1})^* \nabla \psi_h^{n-1} - \psi_h^{n-1} \nabla (\psi_h^{n-1})^*, \mathbf{v}_h), \quad \forall \mathbf{v}_h \in \mathring{\mathbf{U}}_h^r, \end{aligned} \quad (2.12)$$

where $r \geq 0$ and $\widehat{r} = \max\{1, r\}$. $\psi_h^0 = \pi_h \psi_0$ and $\mathbf{A}_h^0 = \pi_h \mathbf{A}_0$ are used at the initial time step.

The linearized backward Euler Galerkin-mixed FEM scheme (2.10)-(2.12) is uncoupled and ψ_h^n and $(\boldsymbol{\sigma}_h^n, \mathbf{A}_h^n)$ can be solved simultaneously. Moreover, for each FEM equation, one only needs to solve a linear system at each time step.

Remark 2.1 A linearized Galerkin-mixed FEM in two dimensional space: *If the superconductor is a long cylinder in the z -direction with a finite cross section and the external applied field $\mathbf{H}_e = H_e[0, 0, 1]^T$ (i.e., \mathbf{H}_e is parallel to the z -axis), the original three dimensional equations (1.1)-(1.2) can be reduced to a two dimensional equation [28, 37]*

$$\frac{\partial \psi}{\partial t} - i\kappa(\text{div} \mathbf{A})\psi + (\frac{i}{\kappa} \nabla + \mathbf{A})^2 \psi + (|\psi|^2 - 1)\psi = 0, \quad (2.13)$$

$$\frac{\partial \mathbf{A}}{\partial t} - \nabla \text{div} \mathbf{A} + \mathbf{curl} \text{curl} \mathbf{A} + \frac{i}{2\kappa} (\psi^* \nabla \psi - \psi \nabla \psi^*) + |\psi|^2 \mathbf{A} = \mathbf{curl} H_e, \quad (2.14)$$

with boundary and initial conditions

$$\frac{\partial \psi}{\partial \mathbf{n}} = 0, \quad \operatorname{curl} \mathbf{A} = H_e, \quad \mathbf{A} \cdot \mathbf{n} = 0, \quad \text{on } \partial\Omega \times (0, T], \quad (2.15)$$

$$\psi(x, 0) = \psi_0(x), \quad \mathbf{A}(x, 0) = \mathbf{A}_0(x), \quad \text{in } \Omega, \quad (2.16)$$

where ψ and $\mathbf{A} = [A_1, A_2]^T$ are scalar-valued complex function and vector-valued real function, respectively. The operators div , ∇ , curl and \mathbf{curl} in (2.13)-(2.16) are defined by

$$\operatorname{div} \mathbf{A} = \frac{\partial A_1}{\partial x} + \frac{\partial A_2}{\partial y}, \quad \nabla \psi = \left[\frac{\partial \psi}{\partial x}, \frac{\partial \psi}{\partial y} \right]^T, \quad \operatorname{curl} \mathbf{A} = \frac{\partial A_2}{\partial x} - \frac{\partial A_1}{\partial y}, \quad \mathbf{curl} \psi = \left[\frac{\partial \psi}{\partial y}, -\frac{\partial \psi}{\partial x} \right]^T.$$

To introduce the FEM scheme for (2.13)-(2.16), for a quasi-uniform triangular mesh \mathcal{T}_h with mesh size $h = \max_{\Omega_K \in \mathcal{T}_h} \{\operatorname{diam} \Omega_K\}$, we denote by \mathcal{V}_h^r and \mathbf{Q}_h^r the r -th order Lagrange finite element subspaces of $\mathcal{H}^1(\Omega)$ and $H^1(\Omega)$, respectively. We also define $\mathring{\mathbf{Q}}_h^r = \mathbf{Q}_h^r \cap \mathring{H}^1(\Omega)$. Let $\mathring{\mathbf{U}}_h^r$ be the r -order Raviart–Thomas finite element subspaces of $\mathring{\mathbf{H}}(\operatorname{div})$, where the case $r = 0$ corresponds to the lowest order Raviart–Thomas element (3 dofs). Then, by introducing $\sigma = \operatorname{curl} \mathbf{A}$, the linearized backward Euler Galerkin-mixed FEM scheme is to find $\psi_h^n \in \mathcal{V}_h^r$ and $(\sigma_h^n, \mathbf{A}_h^n) \in \mathbf{Q}_h^{r+1} \times \mathring{\mathbf{U}}_h^r$, where $\sigma_h^n = \pi_h H_e^n$ on $\partial\Omega$, such that for $n = 1, 2, \dots, N$

$$\begin{aligned} (D_\tau \psi_h^n, \omega_h) - i\kappa((\operatorname{div} \mathbf{A}_h^{n-1})\psi_h^n, \omega_h) + \left(\left(\frac{i}{\kappa} \nabla + \mathbf{A}_h^{n-1} \right) \psi_h^n, \left(\frac{i}{\kappa} \nabla + \mathbf{A}_h^{n-1} \right) \omega_h \right) \\ + (|\psi_h^{n-1}|^2 - 1)\psi_h^n, \omega_h) = 0, \quad \forall \omega_h \in \mathcal{V}_h^r \end{aligned} \quad (2.17)$$

and

$$(\sigma_h^n, \chi_h) - (\mathbf{curl} \chi_h, \mathbf{A}_h^n) = 0, \quad \forall \chi_h \in \mathring{\mathbf{Q}}_h^{r+1}, \quad (2.18)$$

$$\begin{aligned} (D_\tau \mathbf{A}_h^n, \mathbf{v}_h) + (\operatorname{div} \mathbf{A}_h^n, \operatorname{div} \mathbf{v}_h) + (\mathbf{curl} \sigma_h^n, \mathbf{v}_h) + (|\psi_h^{n-1}|^2 \mathbf{A}_h^n, \mathbf{v}_h) \\ = (\mathbf{curl} H_e^n, \mathbf{v}_h) - \frac{i}{2\kappa} ((\psi_h^{n-1})^* \nabla \psi_h^{n-1} - \psi_h^{n-1} \nabla (\psi_h^{n-1})^*, \mathbf{v}_h), \quad \forall \mathbf{v}_h \in \mathring{\mathbf{U}}_h^r, \end{aligned} \quad (2.19)$$

where $\psi_h^0 = \pi_h \psi_0$ and $\mathbf{A}_h^0 = \pi_h \mathbf{A}_0$ are used at the initial time step.

Here we focus our attention on analysis of the mixed scheme and present our main results on optimal error estimates in the following theorem. The proof for the problem in three dimensional space will be given in sections 3 and 4. The proof for the two-dimensional model can be obtained analogously and therefore, omitted here. Numerical simulations on a slightly different scheme were given in [22]. Further comparison with conventional Galerkin FEMs will be presented in the section 5. We assume that the initial-boundary value problem (1.1)-(1.4) has a unique solution satisfying the regularity

$$\psi \in L^\infty(0, T; \mathcal{H}^{l+1}), \quad \psi_t \in L^\infty(0, T; \mathcal{H}^{l+1}), \quad \psi_{tt} \in L^\infty(0, T; \mathcal{L}^2) \quad (2.20)$$

and

$$\begin{cases} \mathbf{A} \in L^\infty(0, T; \mathbf{H}^l), \quad \mathbf{A}_t \in L^\infty(0, T; \mathbf{H}^l), \quad \mathbf{A}_{tt} \in L^\infty(0, T; \mathbf{L}^2), \\ \operatorname{div} \mathbf{A} \in L^\infty(0, T; H^{l+1}), \quad (\operatorname{div} \mathbf{A})_t \in L^\infty(0, T; H^{l+1}), \\ \boldsymbol{\sigma} \in L^\infty(0, T; \mathbf{H}^{l+1}), \quad \boldsymbol{\sigma}_t \in L^\infty(0, T; \mathbf{H}^{l+1}), \end{cases} \quad (2.21)$$

where $l > \frac{1}{2}$ depends on the regularity of the domain Ω .

Theorem 2.2 *Under the assumption (2.20)-(2.21), there exist two positive constants h_0 and τ_0 such that when $h < h_0$ and $\tau < \tau_0$, the FEM systems (2.10)-(2.12) and (2.17)-(2.19) are uniquely solvable and the following error estimate holds*

$$\max_{0 \leq n \leq N} \left(\|\psi_h^n - \psi^n\|_{L^2}^2 + \|\mathbf{A}_h^n - \mathbf{A}^n\|_{L^2}^2 \right) + \tau \sum_{m=0}^N \|\boldsymbol{\sigma}_h^m - \mathbf{curl} \mathbf{A}^m\|_{L^2}^2 \leq C_*(\tau^2 + h^{2s}), \quad (2.22)$$

where $s = \min\{r + 1, l\}$ and C_* is a positive constant independent of n , h and τ .

Remark 2.3 *The above theorem shows that the convergence rate of the mixed method depends upon the order of the FEM spaces and also the regularity of the exact solution. In [31], the authors proved that on a nonconvex polygon, the TDGL equations possess regularity only with $\frac{1}{2} < l < \frac{\pi}{\max_j \omega_j} < 1$, where $\max_j \omega_j$ denotes the largest interior angle of the polygon. More precisely, the two dimensional TDGL equations admit a solution with $l < \frac{2}{3}$ on an L-shape domain. Therefore, the L^2 -norm convergence rate of the Galerkin-mixed method for the problem on an L-shape domain is $O(\tau + h^{2/3-\epsilon})$. We note that the convective Lagrange FEMs converge to a wrong solution due to the fact that in space $\mathbf{A} \in \mathbf{H}^l$ with $l < 1$ on a nonconvex domain, see Example 5.2 in section 5. Analysis for the TDGL equations in certain three-dimensional geometries was given in [30]*

In the rest part of this paper, we denote by C a generic positive constant and ϵ a generic small positive constant, which are independent of C_* , n , h and τ . We present the Gagliardo–Nirenberg inequality in the following lemma which will be frequently used in our proofs.

Lemma 2.4 (*Gagliardo–Nirenberg inequality [36]*): *Let u be a function defined on Ω in \mathbb{R}^d and $\partial^s u$ be any partial derivative of u of order s , then*

$$\|\partial^j u\|_{L^p} \leq C \|\partial^m u\|_{L^r}^a \|u\|_{L^q}^{1-a} + C \|u\|_{L^q},$$

for $0 \leq j < m$ and $\frac{j}{m} \leq a \leq 1$ with

$$\frac{1}{p} = \frac{j}{d} + a \left(\frac{1}{r} - \frac{m}{d} \right) + (1-a) \frac{1}{q},$$

except $1 < r < \infty$ and $m - j - \frac{n}{r}$ is a non-negative integer, in which case the above estimate holds only for $\frac{j}{m} \leq a < 1$.

3 Preliminaries

3.1 An auxiliary elliptic problem

We consider the elliptic boundary value problem

$$\mathbf{curl} \mathbf{curl} \mathbf{u} - \nabla \operatorname{div} \mathbf{u} = \mathbf{f} \quad \text{in } \Omega, \quad (3.1)$$

$$\mathbf{curl} \mathbf{u} \times \mathbf{n} = \mathbf{0}, \quad \mathbf{u} \cdot \mathbf{n} = 0 \quad \text{on } \partial\Omega, \quad (3.2)$$

where $\mathbf{u} = [u_1, u_2, u_3]^T$ and $\mathbf{f} = [f_1, f_2, f_3]^T$. By noting the definition of the standard three dimensional operators \mathbf{curl} , ∇ and div , it is easy to verify that $\mathbf{curl} \mathbf{curl} \mathbf{u} - \nabla \operatorname{div} \mathbf{u} = -\Delta \mathbf{u}$.

By introducing the new variable $\boldsymbol{\sigma} = \mathbf{curl} \mathbf{u}$, the mixed formulation of (3.1) with the boundary condition (3.2) is given by

$$\boldsymbol{\sigma} = \mathbf{curl} \mathbf{u} \quad \text{in } \Omega, \quad (3.3)$$

$$\mathbf{curl} \boldsymbol{\sigma} - \nabla \operatorname{div} \mathbf{u} = \mathbf{f} \quad \text{in } \Omega, \quad (3.4)$$

$$\boldsymbol{\sigma} \times \mathbf{n} = \mathbf{0}, \quad \mathbf{u} \cdot \mathbf{n} = 0 \quad \text{on } \partial\Omega. \quad (3.5)$$

Then, the weak formulation of the above equation is to find $(\boldsymbol{\sigma}, \mathbf{u}) \in \mathring{\mathbf{H}}(\mathbf{curl}) \times \mathring{\mathbf{H}}(\operatorname{div})$, such that

$$(\boldsymbol{\sigma}, \boldsymbol{\chi}) - (\mathbf{curl} \boldsymbol{\chi}, \mathbf{u}) = 0, \quad \forall \boldsymbol{\chi} \in \mathring{\mathbf{H}}(\mathbf{curl}), \quad (3.6)$$

$$(\mathbf{curl} \boldsymbol{\sigma}, \mathbf{v}) + (\operatorname{div} \mathbf{u}, \operatorname{div} \mathbf{v}) = (\mathbf{f}, \mathbf{v}), \quad \forall \mathbf{v} \in \mathring{\mathbf{H}}(\operatorname{div}). \quad (3.7)$$

Based on the above mixed weak formulation, the mixed FEM approximation to (3.6)-(3.7) is to find $(\boldsymbol{\sigma}_h, \mathbf{u}_h) \in \mathring{\mathbf{Q}}_h^{r+1} \times \mathring{\mathbf{U}}_h^r$, such that

$$(\boldsymbol{\sigma}_h, \boldsymbol{\chi}_h) - (\mathbf{curl} \boldsymbol{\chi}_h, \mathbf{u}_h) = 0, \quad \forall \boldsymbol{\chi}_h \in \mathring{\mathbf{Q}}_h^{r+1}, \quad (3.8)$$

$$(\mathbf{curl} \boldsymbol{\sigma}_h, \mathbf{v}_h) + (\operatorname{div} \mathbf{u}_h, \operatorname{div} \mathbf{v}_h) = (\mathbf{f}, \mathbf{v}_h), \quad \forall \mathbf{v}_h \in \mathring{\mathbf{U}}_h^r. \quad (3.9)$$

Theoretical analysis on convergence and stability of the above mixed finite element methods can be found in the two seminal papers [4, 5], while our main concern in this paper is on the nonlinear parabolic problem of superconductivity. We summarize the main results in the following lemma and we refer to [4, 5] for details.

Lemma 3.1 *Let $(\boldsymbol{\sigma}, \mathbf{u})$ and $(\boldsymbol{\sigma}_h, \mathbf{u}_h)$ be the solution of (3.6)-(3.7) and (3.8)-(3.9), respectively. Then the following error estimates hold*

$$\begin{aligned} & \|\boldsymbol{\sigma} - \boldsymbol{\sigma}_h\|_{\mathbf{H}(\mathbf{curl})} + \|\mathbf{u} - \mathbf{u}_h\|_{\mathbf{H}(\operatorname{div})} \\ & \leq C \left(\inf_{\boldsymbol{\chi}_h \in \mathring{\mathbf{Q}}_h^{r+1}} \|\boldsymbol{\sigma} - \boldsymbol{\chi}_h\|_{\mathbf{H}(\mathbf{curl})} + \inf_{\mathbf{v}_h \in \mathring{\mathbf{U}}_h^r} \|\mathbf{u} - \mathbf{v}_h\|_{\mathbf{H}(\operatorname{div})} \right) \end{aligned} \quad (3.10)$$

3.2 Elliptic and mixed projections

To prove the optimal error estimates of the linearized Galerkin-mixed FEM scheme (2.10)-(2.12), we define a Ritz projection operator $R_h : \mathcal{H}^1(\Omega) \rightarrow \mathcal{V}_h^{\widehat{r}}$ and a mixed projection operator $\mathbf{P}_h : \mathbf{H}(\mathbf{curl}) \times \mathring{\mathbf{H}}(\operatorname{div}) \rightarrow \mathring{\mathbf{Q}}_h^{r+1} \times \mathring{\mathbf{U}}_h^r$ as follows (also see [40]): for given $t \in [0, T]$, find $R_h \psi \in \mathcal{V}_h^{\widehat{r}}$ and $\mathbf{P}_h(\boldsymbol{\sigma}, \mathbf{A}) := (P_h^1(\boldsymbol{\sigma}, \mathbf{A}), P_h^2(\boldsymbol{\sigma}, \mathbf{A})) \in \mathring{\mathbf{Q}}_h^{r+1} \times \mathring{\mathbf{U}}_h^r$ with $P_h^1(\boldsymbol{\sigma}, \mathbf{A}) \times \mathbf{n} = \pi_h \boldsymbol{\sigma} \times \mathbf{n}$ on $\partial\Omega$, such that

$$\frac{1}{\kappa^2} (\nabla(\psi - R_h \psi), \nabla \omega_h) + M(\psi - R_h \psi, \omega_h) = 0, \quad \forall \omega_h \in \mathcal{V}_h^{\widehat{r}} \quad (3.11)$$

where M is a positive constant which is chosen to ensure the coercivity of (3.11) and

$$(\boldsymbol{\sigma} - P_h^1(\boldsymbol{\sigma}, \mathbf{A}), \boldsymbol{\chi}_h) - (\mathbf{curl} \boldsymbol{\chi}_h, \mathbf{A} - P_h^2(\boldsymbol{\sigma}, \mathbf{A})) = 0, \quad \forall \boldsymbol{\chi}_h \in \mathring{\mathbf{Q}}_h^{r+1}, \quad (3.12)$$

$$(\mathbf{curl}(\boldsymbol{\sigma} - P_h^1(\boldsymbol{\sigma}, \mathbf{A})), \mathbf{v}_h) + (\operatorname{div}(\mathbf{A} - P_h^2(\boldsymbol{\sigma}, \mathbf{A})), \operatorname{div} \mathbf{v}_h) = 0, \quad \forall \mathbf{v}_h \in \mathring{\mathbf{U}}_h^r. \quad (3.13)$$

We denote the projection error functions by

$$\rho_\psi = R_h \psi - \psi, \quad \rho_\boldsymbol{\sigma} = P_h^1(\boldsymbol{\sigma}, \mathbf{A}) - \boldsymbol{\sigma}, \quad \rho_{\mathbf{A}} = P_h^2(\boldsymbol{\sigma}, \mathbf{A}) - \mathbf{A}.$$

With the regularity assumption (2.20)-(2.21), by standard finite element theory [8] and Lemma 3.1, we have the following error estimates

$$\begin{cases} \|\rho_\psi\|_{L^2} + \|(\rho_\psi)_t\|_{L^2} \leq Ch^{\min\{2l, \hat{r}+1\}}, & \|\rho_\psi\|_{H^1} \leq Ch^{\min\{l, \hat{r}\}}, \\ \|\rho_\sigma\|_{\mathbf{H}(\mathbf{curl})} \leq Ch^s, & \|\rho_{\mathbf{A}}\|_{\mathbf{H}(\mathbf{div})} + \|(\rho_{\mathbf{A}})_t\|_{L^2} \leq Ch^s, \end{cases} \quad (3.14)$$

and the stability result

$$\|R_h\psi\|_{L^\infty} \leq C, \quad \|R_h\psi\|_{W^{1,3}} \leq C. \quad (3.15)$$

4 The proof of Theorem 2.2

For $n = 0, \dots, N$, we denote

$$e_\psi^n = \psi_h^n - R_h\psi^n, \quad e_\sigma^n = \sigma_h^n - P_h^1(\sigma^n, \mathbf{A}^n), \quad e_{\mathbf{A}}^n = \mathbf{A}_h^n - P_h^2(\sigma^n, \mathbf{A}^n).$$

In this section, we prove that the following inequality holds for $n = 0, \dots, N$

$$\|e_\psi^n\|_{L^2}^2 + \|e_{\mathbf{A}}^n\|_{L^2}^2 + \sum_{m=1}^n \tau \left(\|e_\psi^m\|_{H^1}^2 + \|e_\sigma^m\|_{L^2}^2 + \|\operatorname{div} e_{\mathbf{A}}^m\|_{L^2}^2 \right) \leq \frac{C_*}{2} (\tau^2 + h^{2s}) \quad (4.1)$$

by mathematical induction. Theorem 2.2 follows immediately from the the projection error estimates in (3.14) and the above inequality.

Since

$$\|e_\psi^0\|_{L^2}^2 + \|e_{\mathbf{A}}^0\|_{L^2}^2 = \|\pi_h\psi_0 - R_h\psi^0\|_{L^2}^2 + \|\pi_h\mathbf{A}_0 - P_h^2(\sigma^0, \mathbf{A}^0)\|_{L^2}^2 \leq C_1 h^{2s},$$

(4.1) holds for $n = 0$ if we require $\frac{C_*}{2} \geq C_1$, we can assume that (4.1) holds for $n \leq k-1$ for some $k \geq 1$. We shall find a constant C_* , which is independent of n, h, τ , such that (4.1) holds for $n \leq k$. The generic positive constant C in the rest part of this paper is independent of C_* .

From the mixed variational form (2.6)-(2.8), the linearized Galerkin-mixed FEM scheme (2.10)-(2.12), and the projection (3.11)-(3.13), the error functions e_ψ^n, e_σ^n and $e_{\mathbf{A}}^n$ satisfy

$$\begin{aligned} & (D_\tau e_\psi^n, \omega_h) + \frac{1}{\kappa^2} (\nabla e_\psi^n, \nabla \omega_h) + M(e_\psi^n, \omega_h) \\ &= -(D_\tau \rho_\psi^n, \omega_h) + i\kappa \left((\operatorname{div} \mathbf{A}_h^{n-1}) \psi_h^n - (\operatorname{div} \mathbf{A}^{n-1}) \psi^n, \omega_h \right) \\ &+ \frac{i}{\kappa} (\mathbf{A}_h^{n-1} \psi_h^n - \mathbf{A}^{n-1} \psi^n, \nabla \omega_h) - \frac{i}{\kappa} \left((\nabla \psi_h^n, \mathbf{A}_h^{n-1} \omega_h) - (\nabla \psi^n, \mathbf{A}^{n-1} \omega_h) \right) \\ &+ (M\psi_h^n + (1 - |\psi_h^{n-1}|^2 - |\mathbf{A}_h^{n-1}|^2) \psi_h^n - M\psi^n - (1 - |\psi^{n-1}|^2 - |\mathbf{A}^{n-1}|^2) \psi^n, \omega_h) \\ &+ R_\psi^n \\ &= \sum_{i=1}^5 J_i^n(\omega_h) + R_\psi^n, \quad \forall \omega_h \in \mathcal{V}_h^{\hat{r}}, \quad n = 1, 2, \dots, N \end{aligned} \quad (4.2)$$

and

$$(e_{\sigma}^n, \chi_h) - (\mathbf{curl} \chi_h, e_{\mathbf{A}}^n) = 0, \quad \forall \chi_h \in \mathring{\mathbf{Q}}_h^{r+1}, \quad n = 1, 2, \dots, N, \quad (4.3)$$

$$\begin{aligned} & (D_{\tau} e_{\mathbf{A}}^n, \mathbf{v}_h) + (\operatorname{div} e_{\mathbf{A}}^n, \operatorname{div} \mathbf{v}_h) + (\mathbf{curl} e_{\sigma}^n, \mathbf{v}_h) \\ &= -(D_{\tau} \rho_{\mathbf{A}}^n, \mathbf{v}_h) - \frac{i}{2\kappa} [((\psi_h^{n-1})^* \nabla \psi_h^{n-1} - \psi_h^{n-1} \nabla (\psi_h^{n-1})^*), \mathbf{v}_h] \\ & \quad - ((\psi^{n-1})^* \nabla \psi^{n-1} - \psi^{n-1} \nabla (\psi^{n-1})^*), \mathbf{v}_h] \\ & \quad - (|\psi_h^{n-1}|^2 \mathbf{A}_h^n - |\psi^{n-1}|^2 \mathbf{A}^n, \mathbf{v}_h) + R_{\mathbf{A}}^n \\ &= \sum_{i=6}^8 J_i^n(\mathbf{v}_h) + R_{\mathbf{A}}^n, \quad \forall \mathbf{v}_h \in \mathring{\mathbf{U}}_h^r, \quad n = 1, 2, \dots, N, \end{aligned} \quad (4.4)$$

where

$$\begin{aligned} R_{\psi}^n &= (D_{\tau} \psi^n - \frac{\partial \psi(\cdot, t_n)}{\partial t}, \omega_h) + i\kappa (\operatorname{div} (\mathbf{A}^n - \mathbf{A}^{n-1}) \psi^n, \omega_h) \\ & \quad + \frac{i}{\kappa} (\nabla \psi^n, (\mathbf{A}^{n-1} - \mathbf{A}^n) \omega_h) - \frac{i}{\kappa} ((\mathbf{A}^{n-1} - \mathbf{A}^n) \psi^n, \nabla \omega_h) \\ & \quad + ((\mathbf{A}^{n-1}|^2 - |\mathbf{A}^n|^2 + |\psi^{n-1}|^2 - |\psi^n|^2) \psi^n, \omega_h) \end{aligned}$$

and

$$\begin{aligned} R_{\mathbf{A}}^n &= (D_{\tau} \mathbf{A}^n - \frac{\partial \mathbf{A}(\cdot, t_n)}{\partial t}, \mathbf{v}_h) - (|\psi^n|^2 \mathbf{A}^n - |\psi^{n-1}|^2 \mathbf{A}^n, \mathbf{v}_h) \\ & \quad - \frac{i}{2\kappa} (((\psi^n)^* \nabla \psi^n - \psi^n \nabla (\psi^n)^*) - ((\psi^{n-1})^* \nabla \psi^{n-1} - \psi^{n-1} \nabla (\psi^{n-1})^*), \mathbf{v}_h) \end{aligned}$$

define the truncation errors.

We take $\omega_h = e_{\psi}^n$ and $(\chi_h, \mathbf{v}_h) = (e_{\sigma}^n, e_{\mathbf{A}}^n)$ in (4.2)-(4.4), respectively. It is easy to see that, with the regularity assumptions (2.20)-(2.21),

$$|R_{\psi}^n| + |R_{\mathbf{A}}^n| \leq \epsilon \|\nabla e_{\psi}^n\|_{L^2}^2 + C \|e_{\psi}^n\|_{L^2}^2 + C \|e_{\mathbf{A}}^n\|_{L^2}^2 + \epsilon^{-1} C \tau^2. \quad (4.5)$$

We now estimate $J_i^n(e_{\psi}^n)$ for $i = 1, \dots, 5$ in (4.2) and $J_i^n(e_{\mathbf{A}}^n)$ for $i = 6, 7, 8$ in (4.4) term by term. By noting the projection error estimates (3.14), we have

$$\begin{aligned} |J_1^n(e_{\psi}^n)| &\leq C \|e_{\psi}^n\|^2 + Ch^{2s}, \\ |J_6^n(e_{\mathbf{A}}^n)| &\leq C \|e_{\mathbf{A}}^n\|^2 + Ch^{2s} \end{aligned}$$

and

$$\begin{aligned} \mathcal{Re}(J_2^n(e_{\psi}^n)) &= \mathcal{Re}(i\kappa ((\operatorname{div} \mathbf{A}_h^{n-1}) e_{\psi}^n + (\operatorname{div} \mathbf{A}_h^{n-1}) R_h \psi^n - (\operatorname{div} \mathbf{A}^{n-1}) \psi^n, e_{\psi}^n)) \\ &= \mathcal{Re}(i\kappa ((\operatorname{div} \mathbf{A}_h^{n-1}) R_h \psi^n - (\operatorname{div} \mathbf{A}^{n-1}) \psi^n, e_{\psi}^n)) \\ &\leq C |((\operatorname{div} (e_{\mathbf{A}}^{n-1} + \rho_{\mathbf{A}}^{n-1})) R_h \psi^n, e_{\psi}^n)| + C |((\operatorname{div} \mathbf{A}^{n-1}) \rho_{\psi}^n, e_{\psi}^n)| \\ &\leq C (\|\operatorname{div} e_{\mathbf{A}}^{n-1}\|_{L^2} + \|\operatorname{div} \rho_{\mathbf{A}}^{n-1}\|_{L^2}) \|R_h \psi^n\|_{L^{\infty}} \|e_{\psi}^n\|_{L^2} \\ & \quad + C \|\operatorname{div} \mathbf{A}^{n-1}\|_{L^{\infty}} \|\rho_{\psi}^{n-1}\|_{L^2} \|e_{\psi}^n\|_{L^2} \\ &\leq \epsilon \|\operatorname{div} e_{\mathbf{A}}^{n-1}\|_{L^2} + \epsilon^{-1} C (\|e_{\psi}^n\|_{L^2}^2 + h^{2s}), \end{aligned}$$

where $\mathcal{Re}(J_i)$ denotes the real part of J_i and also, we have noted the fact that

$$\mathcal{Re}((i\kappa (\operatorname{div} \mathbf{A}_h^{n-1}) e_{\psi}^n, e_{\psi}^n)) = 0.$$

For the term J_3^n , we see that

$$\begin{aligned}
|\mathcal{R}e(J_3^n(e_\psi^n))| &\leq C|\mathcal{I}m(((e_{\mathbf{A}}^{n-1} + \rho_{\mathbf{A}}^{n-1})\psi_h^n + \mathbf{A}^{n-1}(e_\psi^n + \rho_\psi^n), \nabla e_\psi^n))| \\
&\leq C|\mathcal{I}m(((e_{\mathbf{A}}^{n-1} + \rho_{\mathbf{A}}^{n-1})e_\psi^n, \nabla e_\psi^n))| + C|\mathcal{I}m(((e_{\mathbf{A}}^{n-1} + \rho_{\mathbf{A}}^{n-1})R_h\psi^n, \nabla e_\psi^n))| \\
&\quad + C|\mathcal{I}m((\mathbf{A}^{n-1}(e_\psi^n + \rho_\psi^n), \nabla e_\psi^n))| \\
&\leq C|\mathcal{I}m((e_{\mathbf{A}}^{n-1}e_\psi^n, \nabla e_\psi^n))| + C\|\rho_{\mathbf{A}}^{n-1}\|_{L^2}\|e_\psi^n\|_{L^\infty}\|\nabla e_\psi^n\|_{L^2} + \epsilon\|\nabla e_\psi^n\|_{L^2}^2 \\
&\quad + \epsilon^{-1}C(\|e_\psi^n\|_{L^2}^2 + \|e_{\mathbf{A}}^{n-1}\|_{L^2}^2 + h^{2s}) \\
&\leq C|\mathcal{I}m((e_{\mathbf{A}}^{n-1}e_\psi^n, \nabla e_\psi^n))| + Ch^{s-\frac{1}{2}}\|e_\psi^n\|_{H^1}^2 + \epsilon\|e_\psi^n\|_{H^1}^2 \\
&\quad + \epsilon^{-1}C(\|e_\psi^n\|_{L^2}^2 + \|e_{\mathbf{A}}^{n-1}\|_{L^2}^2 + h^{2s}) \\
&\leq C|\mathcal{I}m((e_{\mathbf{A}}^{n-1}e_\psi^n, \nabla e_\psi^n))| + \epsilon\|e_\psi^n\|_{H^1}^2 + \epsilon^{-1}C(\|e_\psi^n\|_{L^2}^2 + \|e_{\mathbf{A}}^{n-1}\|_{L^2}^2 + h^{2s})
\end{aligned}$$

where we have used the projection error estimate (3.14) and an inverse inequality and required $Ch^{s-\frac{1}{2}} \leq \epsilon$.

Similarly, J_4^n is bounded by

$$\begin{aligned}
|\mathcal{R}e(J_4^n(e_\psi^n))| &\leq C|\mathcal{I}m((\nabla(e_\psi^n + \rho_\psi^n), \mathbf{A}_h^{n-1}e_\psi^n))| + C|\mathcal{I}m((\nabla\psi^n, (e_{\mathbf{A}}^{n-1} + \rho_{\mathbf{A}}^{n-1})e_\psi^n))| \\
&\leq C|\mathcal{I}m((\nabla(e_\psi^n + \rho_\psi^n), (e_{\mathbf{A}}^{n-1} + \rho_{\mathbf{A}}^{n-1})e_\psi^n))| + C|\mathcal{I}m((\nabla(e_\psi^n + \rho_\psi^n), \mathbf{A}^{n-1}e_\psi^n))| \\
&\quad + \epsilon\|e_\psi^n\|_{H^1}^2 + \epsilon^{-1}C(\|e_\psi^n\|_{L^2}^2 + \|e_{\mathbf{A}}^{n-1}\|_{L^2}^2 + h^{2s}).
\end{aligned}$$

By requiring $Ch^{s-\frac{1}{2}} \leq \epsilon$ and using inverse inequalities and integration by parts,

$$\begin{aligned}
|\mathcal{I}m(\nabla\rho_\psi^n, (e_{\mathbf{A}}^{n-1} + \rho_{\mathbf{A}}^{n-1})e_\psi^n)| &\leq \|\nabla\rho_\psi^n\|_{L^3}\|e_{\mathbf{A}}^{n-1} + \rho_{\mathbf{A}}^{n-1}\|_{L^2}\|e_\psi^n\|_{L^6} \\
&\leq C(h^s + \|e_{\mathbf{A}}^{n-1}\|_{L^2})\|e_\psi^n\|_{H^1} \\
&\leq \epsilon\|e_\psi^n\|_{H^1}^2 + C(\|e_{\mathbf{A}}^{n-1}\|_{L^2}^2 + h^{2s}), \\
|\mathcal{I}m((\nabla e_\psi^n, \rho_{\mathbf{A}}^{n-1}e_\psi^n))| &\leq \|\nabla e_\psi^n\|_{L^2}\|\rho_{\mathbf{A}}^{n-1}\|_{L^2}\|e_\psi^n\|_{L^\infty} \leq Ch^{s-\frac{1}{2}}\|e_\psi^n\|_{H^1}^2 \leq \epsilon\|e_\psi^n\|_{H^1}^2, \\
|\mathcal{I}m((\nabla(e_\psi^n + \rho_\psi^n), \mathbf{A}^{n-1}e_\psi^n))| &= |\mathcal{I}m((e_\psi^n + \rho_\psi^n, (\operatorname{div} \mathbf{A}^{n-1})e_\psi^n))| \\
&\quad + |\mathcal{I}m((e_\psi^n + \rho_\psi^n, \mathbf{A}^{n-1} \cdot \nabla e_\psi^n))| \\
&\leq \epsilon\|e_\psi^n\|_{H^1}^2 + \epsilon^{-1}C\|e_\psi^n\|_{L^2}^2 + \epsilon^{-1}Ch^{2s}.
\end{aligned}$$

Then it follows that

$$|\mathcal{R}e(J_4^n(e_\psi^n))| \leq C|\mathcal{I}m((\nabla e_\psi^n, e_{\mathbf{A}}^{n-1}e_\psi^n))| + \epsilon\|e_\psi^n\|_{H^1}^2 + \epsilon^{-1}C(\|e_\psi^n\|_{L^2}^2 + \|e_{\mathbf{A}}^{n-1}\|_{L^2}^2 + h^{2s}).$$

For the term J_5^n , we have the bound

$$\begin{aligned}
\mathcal{R}e(J_5^n(e_\psi^n)) &\leq -\mathcal{R}e((|\psi_h^{n-1}|^2 + |\mathbf{A}_h^{n-1}|^2)\psi_h^n - (|\psi^{n-1}|^2 + |\mathbf{A}^{n-1}|^2)\psi^n, e_\psi^n) \\
&\quad + (M+1)\|e_\psi^n\|_{L^2}^2 + (M+1)(\rho_\psi^n, e_\psi^n).
\end{aligned}$$

Since

$$\begin{aligned}
&-\mathcal{R}e((|\mathbf{A}_h^{n-1}|^2\psi_h^n - |\mathbf{A}^{n-1}|^2\psi^n, e_\psi^n)) \\
&= -(|\mathbf{A}_h^{n-1}|^2e_\psi^n, e_\psi^n) - \mathcal{R}e((|\mathbf{A}_h^{n-1}|^2R_h\psi^n - |\mathbf{A}^{n-1}|^2\psi^n, e_\psi^n)) \\
&\leq -(|\mathbf{A}_h^{n-1}|^2e_\psi^n, e_\psi^n) + |(|\mathbf{A}^{n-1}|^2\rho_\psi^n, e_\psi^n)| + |((|\mathbf{A}_h^{n-1}|^2 - |\mathbf{A}^{n-1}|^2)R_h\psi^n, e_\psi^n)| \\
&\leq -(|\mathbf{A}_h^{n-1}|^2e_\psi^n, e_\psi^n) + |((\mathbf{A}_h^{n-1} + \mathbf{A}^{n-1}) \cdot (e_{\mathbf{A}}^{n-1} + \rho_{\mathbf{A}}^{n-1})R_h\psi^n, e_\psi^n)| \\
&\quad + \epsilon\|e_\psi^n\|_{H^1}^2 + \epsilon^{-1}Ch^{2s} \\
&\leq \epsilon\|e_\psi^n\|_{H^1}^2 + \epsilon^{-1}C(\|e_{\mathbf{A}}^{n-1}\|_{L^2}^2 + h^{2s})
\end{aligned}$$

and

$$-\operatorname{Re}(|\psi_h^{n-1}|^2 \psi_h^n - |\psi^{n-1}|^2 \psi^n, e_\psi^n) \leq \epsilon \|e_\psi^n\|_{H^1}^2 + \epsilon^{-1} C (\|e_\psi^{n-1}\|_{L^2}^2 + h^{2s}),$$

the real part of $J_5^n(e_\psi^n)$ can be bounded by

$$\operatorname{Re}(J_5^n(e_\psi^n)) \leq \epsilon \|e_\psi^n\|_{H^1}^2 + \epsilon^{-1} C (\|e_\psi^{n-1}\|_{L^2}^2 + \|e_{\mathbf{A}}^{n-1}\|_{L^2}^2 + h^{2s}).$$

For J_7^n , we can see that

$$\begin{aligned} J_7^n(e_{\mathbf{A}}^n) &\leq C |\operatorname{Im}((\psi_h^{n-1})^* \nabla \psi_h^{n-1} - (\psi^{n-1})^* \nabla \psi^{n-1}, e_{\mathbf{A}}^n)| \\ &\quad + C |\operatorname{Im}((\psi_h^{n-1} \nabla (\psi_h^{n-1})^* - \psi^{n-1} \nabla (\psi^{n-1})^*), e_{\mathbf{A}}^n)|. \end{aligned} \quad (4.6)$$

Moreover, the first term in the right hand side of (4.6) is bounded by

$$\begin{aligned} &|\operatorname{Im}((\psi_h^{n-1})^* \nabla \psi_h^{n-1} - (\psi^{n-1})^* \nabla \psi^{n-1}, e_{\mathbf{A}}^n)| \\ &= |\operatorname{Im}(((\psi_h^{n-1})^* \nabla (e_\psi^{n-1} + \rho_\psi^{n-1}) + (e_\psi^{n-1} + \rho_\psi^{n-1})^* \nabla \psi^{n-1}, e_{\mathbf{A}}^n))| \\ &\leq C |\operatorname{Im}(((\psi_h^{n-1})^* \nabla (e_\psi^{n-1} + \rho_\psi^{n-1}), e_{\mathbf{A}}^n))| + \epsilon \|e_\psi^{n-1}\|_{H^1}^2 + \epsilon^{-1} C (\|e_{\mathbf{A}}^n\|_{L^2}^2 + h^{2s}) \\ &\leq C |\operatorname{Im}(((e_\psi^{n-1})^* \nabla (e_\psi^{n-1} + \rho_\psi^{n-1}), e_{\mathbf{A}}^n))| + C |\operatorname{Im}(((R_h \psi^{n-1})^* \nabla (e_\psi^{n-1} + \rho_\psi^{n-1}), e_{\mathbf{A}}^n))| \\ &\quad + \epsilon \|e_\psi^{n-1}\|_{H^1}^2 + \epsilon^{-1} C (\|e_{\mathbf{A}}^n\|_{L^2}^2 + h^{2s}) \\ &\leq C |\operatorname{Im}(((e_\psi^{n-1})^* \nabla e_\psi^{n-1}, e_{\mathbf{A}}^n))| + C \|e_\psi^{n-1}\|_{L^\infty} \|\nabla \rho_\psi^{n-1}\|_{L^2} \|e_{\mathbf{A}}^n\|_{L^2} \\ &\quad + C |\operatorname{Im}(((R_h \psi^{n-1})^* \nabla \rho_\psi^{n-1}, e_{\mathbf{A}}^n))| + \epsilon \|e_\psi^{n-1}\|_{H^1}^2 + \epsilon^{-1} C (\|e_{\mathbf{A}}^n\|_{L^2}^2 + \|e_\psi^{n-1}\|_{L^2}^2 + h^{2s}). \\ &\leq C |\operatorname{Im}(((e_\psi^{n-1})^* \nabla e_\psi^{n-1}, e_{\mathbf{A}}^n))| + C h^{s-\frac{1}{2}} \|e_\psi^{n-1}\|_{H^1} \|e_{\mathbf{A}}^n\|_{L^2} \\ &\quad + \epsilon \|\operatorname{div} e_{\mathbf{A}}^n\|_{L^2}^2 + \epsilon \|e_\psi^{n-1}\|_{H^1}^2 + \epsilon^{-1} C (\|e_{\mathbf{A}}^n\|_{L^2}^2 + \|e_\psi^{n-1}\|_{L^2}^2 + h^{2s}). \\ &\leq C |\operatorname{Im}(((e_\psi^{n-1})^* \nabla e_\psi^{n-1}, e_{\mathbf{A}}^n))| + \epsilon \|\operatorname{div} e_{\mathbf{A}}^n\|_{L^2}^2 + \epsilon \|e_\psi^{n-1}\|_{H^1}^2 \\ &\quad + \epsilon^{-1} C (\|e_{\mathbf{A}}^n\|_{L^2}^2 + \|e_\psi^{n-1}\|_{L^2}^2 + h^{2s}), \end{aligned}$$

where we have used an inverse inequality and required that $Ch^{s-\frac{1}{2}} \leq 1$. Similarly, the second term in the right hand side of (4.6) is bounded by

$$\begin{aligned} &C |\operatorname{Im}((\psi_h^{n-1} \nabla (\psi_h^{n-1})^* - \psi^{n-1} \nabla (\psi^{n-1})^*), e_{\mathbf{A}}^n)| \\ &\leq C |\operatorname{Im}((e_\psi^{n-1} \nabla (e_\psi^{n-1})^*), e_{\mathbf{A}}^n)| + \epsilon \|\operatorname{div} e_{\mathbf{A}}^n\|_{L^2}^2 + \epsilon \|e_\psi^{n-1}\|_{H^1}^2 \\ &\quad + \epsilon^{-1} C (\|e_{\mathbf{A}}^n\|_{L^2}^2 + \|e_\psi^{n-1}\|_{L^2}^2 + h^{2s}), \end{aligned}$$

It follows that

$$\begin{aligned} J_7^n(e_{\mathbf{A}}^n) &\leq C |\operatorname{Im}(((e_\psi^{n-1})^* \nabla e_\psi^{n-1}, e_{\mathbf{A}}^n))| + \epsilon \|\operatorname{div} e_{\mathbf{A}}^n\|_{L^2}^2 + \epsilon \|e_\psi^{n-1}\|_{H^1}^2 \\ &\quad + \epsilon^{-1} C (\|e_{\mathbf{A}}^n\|_{L^2}^2 + \|e_\psi^{n-1}\|_{L^2}^2 + h^{2s}). \end{aligned}$$

Finally, for the term J_8^n , we can derive that

$$\begin{aligned} J_8^n(e_{\mathbf{A}}^n) &\leq -(|\psi_h^{n-1}|^2 \mathbf{A}_h^n - |\psi^{n-1}|^2 \mathbf{A}_h^n, e_{\mathbf{A}}^n) + C \|e_{\mathbf{A}}^n\|_{L^2}^2 + Ch^{2s} \\ &= -(|\psi_h^{n-1}|^2 e_{\mathbf{A}}^n, e_{\mathbf{A}}^n) - (|\psi_h^{n-1}|^2 P_h^2(\boldsymbol{\sigma}^n, \mathbf{A}^n) - |\psi^{n-1}|^2 \mathbf{A}_h^n, e_{\mathbf{A}}^n) + C \|e_{\mathbf{A}}^n\|_{L^2}^2 + Ch^{2s} \\ &\leq -(|\psi_h^{n-1}|^2 e_{\mathbf{A}}^n, e_{\mathbf{A}}^n) + C |((\psi_h^{n-1} + \psi^{n-1})(e_\psi^{n-1} + \rho_\psi^{n-1}) P_h^2(\boldsymbol{\sigma}^n, \mathbf{A}^n), e_{\mathbf{A}}^n)| \\ &\quad + C \|e_{\mathbf{A}}^n\|_{L^2}^2 + Ch^{2s} \\ &\leq \epsilon \|e_\psi^{n-1}\|_{H^1}^2 + \epsilon^{-1} C (\|e_{\mathbf{A}}^n\|_{L^2}^2 + \|e_\psi^{n-1}\|_{L^2}^2 + h^{2s}). \end{aligned} \quad (4.7)$$

With (4.5) and above estimates for J_i , for $i = 1, \dots, 8$, adding (4.3), (4.4) and the real part of (4.2) together, we get

$$\begin{aligned}
& \mathcal{R}e((D_\tau e_\psi^n, e_\psi^n)) + (D_\tau e_{\mathbf{A}}^n, e_{\mathbf{A}}^n) + \frac{1}{\kappa^2} \|\nabla e_\psi^n\|_{L^2}^2 + \|\operatorname{div} e_{\mathbf{A}}^n\|_{L^2}^2 + \|e_\sigma^n\|_{L^2}^2 \\
& \leq C |\mathcal{I}m(((e_\psi^{n-1})^* \nabla e_\psi^{n-1}, e_{\mathbf{A}}^n))| + C |\mathcal{I}m((e_{\mathbf{A}}^{n-1} e_\psi^n, \nabla e_\psi^n))| \\
& \quad + \epsilon (\|\operatorname{div} e_{\mathbf{A}}^n\|_{L^2}^2 + \|\operatorname{div} e_{\mathbf{A}}^{n-1}\|_{L^2}^2 + \|e_\psi^n\|_{H^1}^2 + \|e_\psi^{n-1}\|_{H^1}^2) \\
& \quad + \epsilon^{-1} C (\|e_\psi^n\|_{L^2}^2 + \|e_\psi^{n-1}\|_{L^2}^2 + \|e_{\mathbf{A}}^n\|_{L^2}^2 + \|e_{\mathbf{A}}^{n-1}\|_{L^2}^2 + \tau^2 + h^{2s}), \tag{4.8}
\end{aligned}$$

for $n = 1, \dots, k$.

In order to estimate $|\mathcal{I}m(((e_\psi^{n-1})^* \nabla e_\psi^{n-1}, e_{\mathbf{A}}^n))|$ and $|\mathcal{I}m((e_{\mathbf{A}}^{n-1} e_\psi^n, \nabla e_\psi^n))|$ in (4.8), we use the induction assumption (4.1) for $n \leq k-1$ and inverse inequalities.

For $\tau \leq h^s$, we have

$$\begin{aligned}
|\mathcal{I}m(((e_\psi^{n-1})^* \nabla e_\psi^{n-1}, e_{\mathbf{A}}^n))| & \leq C \|\nabla e_\psi^{n-1}\|_{L^2} \|e_\psi^{n-1}\|_{L^6} \|e_{\mathbf{A}}^n\|_{L^3} \\
& \leq C \|e_\psi^{n-1}\|_{H^1}^2 h^{-\frac{1}{2}} \|e_{\mathbf{A}}^n\|_{L^2}. \tag{4.9}
\end{aligned}$$

To estimate $\|e_{\mathbf{A}}^n\|_{L^2}$, from (4.4) and estimates (4.7), we have that

$$\begin{aligned}
& \|e_{\mathbf{A}}^n\|_{L^2}^2 + \tau \left(\|e_\sigma^m\|_{L^2}^2 + \|\operatorname{div} e_{\mathbf{A}}^m\|_{L^2}^2 \right) \\
& \leq \|e_{\mathbf{A}}^{n-1}\|_{L^2}^2 + \tau C \|e_\psi^{n-1}\|_{H^1}^2 h^{-\frac{1}{2}} \|e_{\mathbf{A}}^n\|_{L^2} \\
& \quad + \tau (\epsilon \|e_\psi^{n-1}\|_{H^1}^2 + \epsilon^{-1} C (\|e_{\mathbf{A}}^n\|_{L^2}^2 + \|e_\psi^{n-1}\|_{L^2}^2 + \tau^2 + h^{2s})) \\
& \leq \left(\frac{1}{4} + C\tau \right) \|e_{\mathbf{A}}^n\|_{L^2}^2 + \|e_{\mathbf{A}}^{n-1}\|_{L^2}^2 + \tau^2 C \|e_\psi^{n-1}\|_{H^1}^4 h^{-1} + CC_* h^{2s} \\
& \leq \frac{1}{2} \|e_{\mathbf{A}}^n\|_{L^2}^2 + CC_* h^{2s}.
\end{aligned}$$

where $C\tau \leq \frac{1}{4}$. Then substituting the last estimate into (4.9) gives

$$\begin{aligned}
|\mathcal{I}m(((e_\psi^{n-1})^* \nabla e_\psi^{n-1}, e_{\mathbf{A}}^n))| & \leq C \sqrt{C_*} h^{s-\frac{1}{2}} \|e_\psi^{n-1}\|_{H^1}^2 \\
& \leq \epsilon \|e_\psi^{n-1}\|_{H^1}^2 \tag{4.10}
\end{aligned}$$

where we require $C \sqrt{C_*} h^{s-\frac{1}{2}} \leq \epsilon$. Similarly,

$$\begin{aligned}
C |\mathcal{I}m((e_{\mathbf{A}}^{n-1} e_\psi^n, \nabla e_\psi^n))| & \leq C \|e_{\mathbf{A}}^{n-1}\|_{L^3} \|\nabla e_\psi^n\|_{L^2} \|e_\psi^n\|_{L^6} \\
& \leq C \|e_{\mathbf{A}}^{n-1}\|_{L^3} \|\nabla e_\psi^n\|_{L^2}^2 \\
& \leq C h^{-\frac{1}{2}} \|e_{\mathbf{A}}^{n-1}\|_{L^2} \|\nabla e_\psi^n\|_{L^2}^2 \\
& \leq C h^{-\frac{1}{2}} \sqrt{\frac{C_*}{2}} (\tau^2 + h^{2s}) \|\nabla e_\psi^n\|_{L^2}^2 \\
& \leq C \sqrt{C_*} h^{s-\frac{1}{2}} \|\nabla e_\psi^n\|_{L^2}^2 \\
& \leq \epsilon \|\nabla e_\psi^n\|_{L^2}^2 \tag{4.11}
\end{aligned}$$

where h satisfies $C \sqrt{C_*} h^{s-\frac{1}{2}} \leq \epsilon$.

For $h^s \leq \tau$, by (4.1), we have that for $n \leq k-1$

$$\begin{aligned} \|e_\psi^n\|_{L^2}^2 + \|e_{\mathbf{A}}^n\|_{L^2}^2 &\leq \frac{C_*}{2}(\tau^2 + h^{2s}) \leq C_*\tau^2, \\ \|e_\psi^n\|_{H^1}^2 + \|e_\sigma^n\|_{L^2}^2 + \|\operatorname{div} e_{\mathbf{A}}^n\|_{L^2}^2 &\leq \tau^{-1} \frac{C_*}{2}(\tau^2 + h^{2s}) \leq C_*\tau. \end{aligned}$$

Then, we have

$$\begin{aligned} C|\mathcal{I}m(((e_\psi^{n-1})^* \nabla e_\psi^{n-1}, e_{\mathbf{A}}^n))| &\leq C\|e_{\mathbf{A}}^n\|_{L^3}\|e_\psi^{n-1}\|_{H^1}\|e_\psi^{n-1}\|_{L^6} \\ &\leq C\sqrt{C_*\tau}(\|e_\sigma^n\|_{L^2} + \|\operatorname{div} e_{\mathbf{A}}^n\|_{L^2})\|e_\psi^{n-1}\|_{H^1} \\ &\leq \epsilon(\|e_\sigma^n\|_{L^2}^2 + \|\operatorname{div} e_{\mathbf{A}}^n\|_{L^2}^2 + \|e_\psi^{n-1}\|_{H^1}^2) \end{aligned}$$

where τ satisfies $CC_*\tau \leq \epsilon$ and we used the following discrete embedding inequality (the proof is given in appendix)

$$\|e_{\mathbf{A}}^n\|_{L^3} \leq C(\|e_\sigma^n\|_{L^2}^2 + \|\operatorname{div} e_{\mathbf{A}}^n\|_{L^2}^2). \quad (4.12)$$

By noting (4.11) and (4.12), we have

$$\begin{aligned} C|\mathcal{I}m((e_{\mathbf{A}}^{n-1} e_\psi^n, \nabla e_\psi^n))| &\leq C\|e_{\mathbf{A}}^{n-1}\|_{L^3}\|e_\psi^n\|_{H^1}^2 \\ &\leq C(\|e_\sigma^{n-1}\|_{L^2} + \|\operatorname{div} e_{\mathbf{A}}^{n-1}\|_{L^2})\|e_\psi^n\|_{H^1}^2 \\ &\leq C\sqrt{C_*\tau}\|e_\psi^n\|_{H^1}^2 \\ &\leq \epsilon\|e_\psi^n\|_{H^1}^2 \end{aligned}$$

where we require that τ satisfies $C\sqrt{C_*}\tau \leq \epsilon$.

Therefore, from (4.8), for both cases $\tau \leq h^s$ and $h^s \leq \tau$, we can derive that

$$\begin{aligned} \mathcal{R}e((D_\tau e_\psi^n, e_\psi^n)) + (D_\tau e_{\mathbf{A}}^n, e_{\mathbf{A}}^n) + \frac{1}{\kappa^2}\|\nabla e_\psi^n\|_{L^2}^2 + M\|e_\psi^n\|_{L^2}^2 + \|\operatorname{div} e_{\mathbf{A}}^n\|_{L^2}^2 + \|e_\sigma^n\|_{L^2}^2 \\ \leq \epsilon(\|e_\sigma^n\|_{L^2}^2 + \|\operatorname{div} e_{\mathbf{A}}^n\|_{L^2}^2 + \|e_\psi^n\|_{H^1}^2 + \|e_\psi^{n-1}\|_{H^1}^2) \\ + \epsilon^{-1}C(\|e_\psi^n\|_{L^2}^2 + \|e_\psi^{n-1}\|_{L^2}^2 + \|e_{\mathbf{A}}^n\|_{L^2}^2 + \|e_{\mathbf{A}}^{n-1}\|_{L^2}^2 + \tau^2 + h^{2s}). \end{aligned}$$

By choosing a small ϵ and summing up the last inequality from 1 to n , we arrive at

$$\begin{aligned} \|e_\psi^n\|_{L^2}^2 + \|e_{\mathbf{A}}^n\|_{L^2}^2 + \tau \sum_{m=1}^n (\|e_\psi^m\|_{H^1}^2 + \|\operatorname{div} e_{\mathbf{A}}^m\|_{L^2}^2 + \|e_\sigma^m\|_{L^2}^2) \\ \leq C\tau \sum_{m=1}^n (\|e_\psi^m\|_{L^2}^2 + \|e_{\mathbf{A}}^m\|_{L^2}^2) + C(\tau^2 + h^{2s}). \end{aligned}$$

With the help of the Gronwall's inequality, we can deduce that

$$\|e_\psi^n\|_{L^2}^2 + \|e_{\mathbf{A}}^n\|_{L^2}^2 + \sum_{m=1}^n \tau (\|e_\psi^m\|_{H^1}^2 + \|e_\sigma^m\|_{L^2}^2 + \|\operatorname{div} e_{\mathbf{A}}^m\|_{L^2}^2) \leq C(\tau^2 + h^{2s}).$$

Thus (4.1) holds for $n = k$, if we take $C_* > 2C$. The induction is closed and the proof of Theorem 2.2 is complete. \blacksquare

5 Numerical results

In this section, we provide several numerical examples in both two and three dimensional spaces to confirm our theoretical analysis and show the efficiency of the linearized Galerkin-mixed FEM scheme. The computations are carried out with the free software FEniCS [33].

5.1 Two dimensional numerical experiments

Example 5.1 In this example, we consider the following two dimensional artificial problem

$$\frac{\partial \psi}{\partial t} - i\kappa(\operatorname{div} \mathbf{A})\psi + \left(\frac{i}{\kappa}\nabla + \mathbf{A}\right)^2\psi + (|\psi|^2 - 1)\psi = g, \quad (5.1)$$

$$\frac{\partial \mathbf{A}}{\partial t} - \nabla \operatorname{div} \mathbf{A} + \operatorname{curl} \operatorname{curl} \mathbf{A} + \frac{i}{2\kappa}(\psi^* \nabla \psi - \psi \nabla \psi^*) + |\psi|^2 \mathbf{A} = \operatorname{curl} H_e + \mathbf{f}, \quad (5.2)$$

for $t \in (0, T]$, $x \in \Omega$, with boundary and initial conditions

$$\begin{aligned} \frac{\partial \psi}{\partial n} &= 0, \quad \operatorname{curl} \mathbf{A} = H_e, \quad \mathbf{A} \cdot \mathbf{n} = 0, && \text{on } \partial\Omega, \\ \psi(x, 0) &= \psi_0(x), \quad \mathbf{A}(x, 0) = \mathbf{A}_0(x), && \text{in } \Omega, \end{aligned}$$

where $\Omega = (0, 1) \times (0, 1)$ and $\kappa = 1$. The functions \mathbf{f} , g , ψ_0 and \mathbf{A}_0 are chosen correspondingly to the exact solution

$$\psi = \exp(-t)(\cos(\pi x) + i \cos(\pi y)), \quad \mathbf{A} = \begin{bmatrix} \exp(y-t) \sin(\pi x) \\ \exp(x-t) \sin(\pi y) \end{bmatrix}$$

with

$$H_e = \exp(x-t) \sin(\pi y) - \exp(y-t) \sin(\pi x).$$

We set $T = 1.0$ in this example.

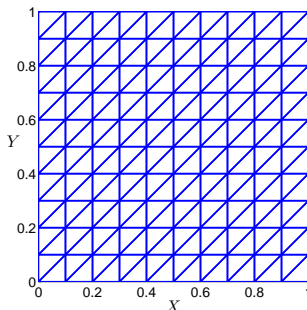


Figure 1: A uniform mesh on the unit square with $M = 10$ (Example 5.1).

We use a uniform triangular partition with $M + 1$ vertices in each direction, see Figure 1 for $M = 10$, where $h = \frac{\sqrt{2}}{M}$. We solve the system (5.1)-(5.2) by the proposed linearized backward Euler Galerkin-mixed finite element methods (2.17)-(2.19) with $(\mathcal{V}_h^r, \mathbf{Q}_h^{r+1} \times \mathbf{U}_h^r)$ for $r = 0, 1, 2$. As $\sigma = \operatorname{curl} \mathbf{A}$ is a real scalar function in the two dimensional case, correspondingly its approximation space \mathbf{Q}_h^{r+1} is the Lagrange element space consisting of all piecewise polynomials up to $(r + 1)$ -th order. As the exact solution is smooth, to confirm our L^2 -norm error estimates,

Table 1: L^2 -norm errors of ψ , \mathbf{A} and σ on the unit square (Example 5.1)..

$(\mathcal{V}_h^1, \mathbf{Q}_h^1 \times \mathbf{U}_h^0)$ $\tau = \frac{1}{M}$	$\ \psi_h^N - \psi(\cdot, t_N)\ _{L^2}$	$\ \mathbf{A}_h^N - \mathbf{A}(\cdot, t_N)\ _{L^2}$	$\ \sigma_h^N - \sigma(\cdot, t_N)\ _{L^2}$
$M = 64$	3.1216e-02	1.0296e-02	2.0804e-03
$M = 128$	1.6284e-02	5.1766e-03	1.0637e-03
$M = 256$	8.3156e-03	2.5959e-03	5.3770e-04
order	0.95	0.99	0.98
$(\mathcal{V}_h^1, \mathbf{Q}_h^2 \times \mathbf{U}_h^1)$ $\tau = \frac{1}{M^2}$	$\ \psi_h^N - \psi(\cdot, t_N)\ _{L^2}$	$\ \mathbf{A}_h^N - \mathbf{A}(\cdot, t_N)\ _{L^2}$	$\ \sigma_h^N - \sigma(\cdot, t_N)\ _{L^2}$
$M = 16$	9.9391e-03	8.1354e-04	6.3113e-04
$M = 32$	2.4956e-03	2.0431e-04	1.5807e-04
$M = 64$	6.2454e-04	5.1132e-05	3.9533e-05
order	2.00	2.00	2.00
$(\mathcal{V}_h^2, \mathbf{Q}_h^3 \times \mathbf{U}_h^2)$ $\tau = \frac{1}{M^3}$	$\ \psi_h^N - \psi(\cdot, t_N)\ _{L^2}$	$\ \mathbf{A}_h^N - \mathbf{A}(\cdot, t_N)\ _{L^2}$	$\ \sigma_h^N - \sigma(\cdot, t_N)\ _{L^2}$
$M = 8$	4.1680e-03	4.5426e-04	2.7586e-04
$M = 16$	5.2687e-04	5.7080e-05	3.4243e-05
$M = 32$	6.6130e-05	7.1400e-06	4.2634e-06
order	2.99	3.00	3.01

we set $\tau = \left(\frac{1}{M}\right)^{r+1}$ in our simulation and we present in Table 1 the L^2 -norm errors of ψ , \mathbf{A} , σ . We can see clearly that the L^2 -norm errors are proportional to h^{r+1} , $r = 0, 1, 2$, which confirm the optimal convergence of the scheme in two dimensional space.

To show the unconditional convergence of the methods, we solve (5.1)-(5.2) by the scheme (2.17)-(2.19) with $(\mathcal{V}_h^1, \mathbf{Q}_h^2 \times \mathbf{U}_h^1)$ and three different time steps $\tau = 0.1, 0.01, 0.001$. For each fixed τ , we take $M = 8, 16, 32, 64, 128$. The L^2 errors of ψ , \mathbf{A} and σ are presented in Figure 2. From Figure 2, we can see that for each fixed τ , when the mesh is refined gradually, each L^2 error converges to a small constant of $O(\tau)$, which shows clearly that the proposed scheme (2.17)-(2.19) is unconditionally stable and no time step restriction is needed.

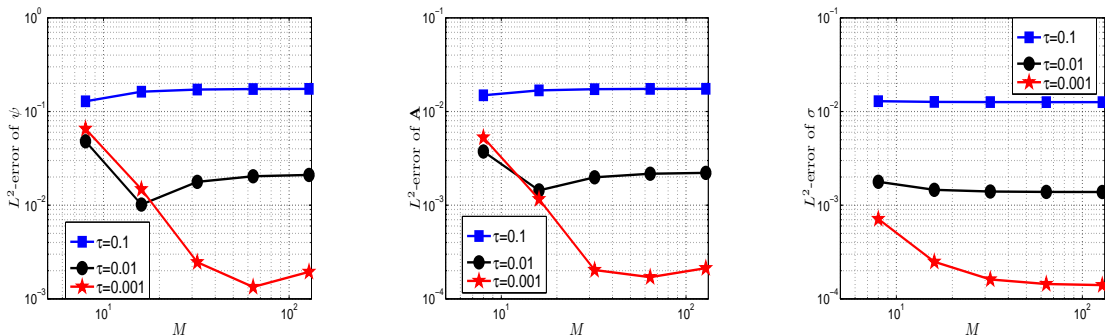


Figure 2: L^2 errors of ψ , \mathbf{A} and σ with $(\mathcal{V}_h^1, \mathbf{Q}_h^2 \times \mathbf{U}_h^1)$ (Example 5.1).

Example 5.2 In this example, we investigate the TDGL equations (5.1)-(5.2) on an L -shape domain with a nonsmooth solution by the Galerkin-mixed method. This example was studied in [31] by a projected FEM based on Hodge decomposition. Here, we use the same exact solution as in [31], i.e., $\kappa = 10$, and the functions \mathbf{f} , g , $H_e = \text{curl } \mathbf{A}$, ψ_0 and \mathbf{A}_0 are chosen correspondingly to the following ψ and \mathbf{A}

$$\psi = t^2 \Phi(r) r^{\frac{2}{3}} \cos\left(\frac{2\theta}{3}\right), \quad \mathbf{A} = \begin{bmatrix} \left(\frac{4}{3}t^2 \Phi(r) r^{-\frac{1}{3}} + t^2 \Phi'(r) r^{\frac{2}{3}}\right) \cos\left(\frac{\theta}{3}\right) \\ \left(\frac{4}{3}t^2 \Phi(r) r^{-\frac{1}{3}} + t^2 \Phi'(r) r^{\frac{2}{3}}\right) \sin\left(\frac{\theta}{3}\right) \end{bmatrix},$$

where (r, θ) denotes the two-dimensional polar coordinates. $\Phi(s)$ in the above expressions is a cut-off function defined by

$$\Phi(s) = \begin{cases} 0.1 & \text{if } s < 0.1, \\ \Upsilon(s) & \text{if } 0.1 \leq s \leq 0.4, \\ 0 & \text{if } s > 0.4, \end{cases}$$

where $\Upsilon(s)$ is a seventh order polynomial satisfying

$$\begin{cases} \Upsilon(0.1) = 0.1, & \Upsilon(0.4) = 0, \\ \Upsilon^{(1)}(0.1) = \Upsilon^{(2)}(0.1) = \Upsilon^{(3)}(0.1) = 0, \\ \Upsilon^{(1)}(0.4) = \Upsilon^{(2)}(0.4) = \Upsilon^{(3)}(0.4) = 0. \end{cases}$$

It is noted that in spatial space, the above exact solution only has the regularity

$$\psi \in \mathcal{H}^{\frac{5}{3}-\epsilon}, \quad \mathbf{A} \in \mathbf{H}^{\frac{2}{3}-\epsilon}, \quad \sigma \in H^{\frac{5}{3}-\epsilon}, \quad \text{div } \mathbf{A} \in H^{\frac{5}{3}-\epsilon}, \quad \text{for } \epsilon > 0.$$

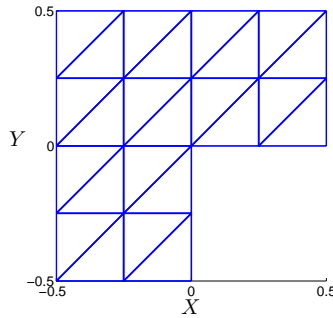


Figure 3: A uniform mesh on the L -shape domain with $M = 4$ (Example 5.2).

Now, we use the Galerkin-mixed method (2.17)-(2.19) to solve the above problem on uniform meshes as shown in Figure 3, where $h = \frac{\sqrt{2}}{M}$. We set the the terminal time $T = 1.0$ and do computation with $(\psi_h, \mathbf{A}_h, \sigma_h) \in (\mathcal{V}_h^1, \mathbf{Q}_h^1, \mathbf{U}_h^0)$ and the time step $\tau = \frac{1}{M}$. The L^2 errors are shown in Table 2. From Table 2, we can see that the convergence rates of the Galerkin-mixed method for the three components ψ , \mathbf{A} and σ , are in the order of $O(h^{1.14})$, $O(h^{0.86})$ and $O(h^{1.91})$, respectively, which indicates that our method is suitable for problems on nonconvex domains.

For comparison, we also solve this artificial problem by a Lagrange type FEM under the same data settings. The linearized backward Euler Lagrange FEM is to find $\psi_h^n \in \mathcal{V}_h^1$ and $\mathbf{A}_h^n \in \mathring{\mathbf{V}}_h^1$,

Table 2: L^2 norm errors of ψ , \mathbf{A} and σ by $(\mathcal{V}_h^1, \mathbf{Q}_h^1 \times \mathbf{U}_h^0)$ on the L -shape domain (Example 5.2).

$(\mathcal{V}_h^1, \mathbf{Q}_h^1 \times \mathbf{U}_h^0)$	$\tau = \frac{1}{M}$	$\ \psi_h^N - \psi(\cdot, t_N)\ _{L^2}$	$\ \mathbf{A}_h^N - \mathbf{A}(\cdot, t_N)\ _{L^2}$	$\ \sigma_h^N - \sigma(\cdot, t_N)\ _{L^2}$
$M = 32$		6.5548e-04	1.7728e-02	1.2104e-01
$M = 64$		2.6140e-04	9.2365e-03	3.3953e-02
$M = 128$		1.2130e-04	5.0878e-03	8.9061e-03
$M = 256$		5.9174e-05	2.9632e-03	2.2696e-03
order		1.04	0.86	1.91

such that for $n = 1, 2, \dots, N$,

$$\begin{aligned} (D_\tau \psi_h^n, \omega_h) - i\kappa((\operatorname{div} \mathbf{A}_h^{n-1})\psi_h^n, \omega_h) + \left(\left(\frac{i}{\kappa} \nabla + \mathbf{A}_h^{n-1} \right) \psi_h^n, \left(\frac{i}{\kappa} \nabla + \mathbf{A}_h^{n-1} \right) \omega_h \right) \\ - ((|\mathbf{A}_h^{n-1}|^2 + |\psi_h^{n-1}|^2 - 1) \psi_h^n, \omega_h) = 0 \quad \forall \omega_h \in \mathcal{V}_h^1, \end{aligned} \quad (5.3)$$

and

$$\begin{aligned} (D_\tau \mathbf{A}_h^n, \mathbf{v}_h) + (\operatorname{div} \mathbf{A}_h^n, \operatorname{div} \mathbf{v}_h) + (\operatorname{curl} \mathbf{A}_h^n, \operatorname{curl} \mathbf{v}_h) + (|\psi_h^{n-1}|^2 \mathbf{A}_h^n, \mathbf{v}_h) \\ = (H_e^n, \operatorname{curl} \mathbf{v}_h) - \frac{i}{2\kappa} ((\psi_h^{n-1})^* \nabla \psi_h^{n-1} - \psi_h^{n-1} \nabla (\psi_h^{n-1})^*, \mathbf{v}_h) \quad \forall \mathbf{v}_h \in \mathring{\mathbf{V}}_h^1, \end{aligned} \quad (5.4)$$

where $\mathring{\mathbf{V}}_h^1$ denotes the linear Lagrange FE subspace of $\{\mathbf{A} \mid \mathbf{A} \in \mathbf{H}^1, \mathbf{A} \cdot \mathbf{n}|_{\partial\Omega} = 0\}$. $\psi_h^0 = \pi_h \psi_0$ and $\mathbf{A}_h^0 = \pi_h \mathbf{A}_0$ are used at the initial time step. The L^2 errors obtained by the conventional Lagrange FEM (5.3)-(5.4) with $M = 32, 64, 128, 256$ are presented in Table 3. We see clearly that the numerical solution of the Lagrange FEM does not converge. We refer to [22, 32] for the numerical observation of the spurious convergence phenomenon by conventional Lagrange FEMs in the vortex motion simulations on an L -shape domain.

Table 3: L^2 norm errors of ψ , \mathbf{A} and σ on the L -shape domain by the conventional Lagrange FEM (5.3)-(5.4) (Example 5.2).

$(\mathcal{V}_h^1, \mathring{\mathbf{V}}_h^1)$	$\tau = \frac{1}{M}$	$\ \psi_h^N - \psi(\cdot, t_N)\ _{L^2}$	$\ \mathbf{A}_h^N - \mathbf{A}(\cdot, t_N)\ _{L^2}$	$\ \sigma_h^N - \sigma(\cdot, t_N)\ _{L^2}$
$M = 32$		3.8735e-03	9.6105e-02	5.1970e-01
$M = 64$		3.8616e-03	9.8059e-02	4.7659e-01
$M = 128$		3.8466e-03	1.0298e-01	4.6553e-01
$M = 256$		3.8395e-03	1.0539e-01	4.6204e-01

5.2 Three dimensional numerical experiments

Numerical results for a three-dimensional artificial example was reported in [22]. For completeness, we include some similar results in this section to confirm the convergence rate of the Galerkin-mixed method for the problems in three-dimensional space.

Example 5.3 We consider the following three dimensional artificial problem

$$\frac{\partial \psi}{\partial t} - i\kappa(\operatorname{div} \mathbf{A})\psi + \left(\frac{i}{\kappa}\nabla + \mathbf{A}\right)^2\psi + (|\psi|^2 - 1)\psi = g, \quad (5.5)$$

$$\frac{\partial \mathbf{A}}{\partial t} - \nabla \operatorname{div} \mathbf{A} + \operatorname{curl} \operatorname{curl} \mathbf{A} + \frac{i}{2\kappa}(\psi^* \nabla \psi - \psi \nabla \psi^*) + |\psi|^2 \mathbf{A} = \operatorname{curl} \mathbf{H}_e + \mathbf{f}, \quad (5.6)$$

for $t \in (0, T]$, $x \in \Omega$, with

$$\begin{aligned} \frac{\partial \psi}{\partial \mathbf{n}} = 0, \quad \operatorname{curl} \mathbf{A} \times \mathbf{n} = \mathbf{H}_e \times \mathbf{n}, \quad \mathbf{A} \cdot \mathbf{n} = 0, & \quad \text{on } \partial\Omega, \\ \psi(x, 0) = \psi_0(x), \quad \mathbf{A}(x, 0) = \mathbf{A}_0(x), & \quad \text{in } \Omega, \end{aligned}$$

where we set $\Omega = (0, 1) \times (0, 1) \times (0, 1)$ and $\kappa = 1$. The functions \mathbf{f} , g , ψ_0 and \mathbf{A}_0 are chosen correspondingly to the exact solution

$$\psi = \exp(t) (\cos(\pi x) \cos(\pi z) + i \cos(\pi y) \cos(\pi z)), \quad \mathbf{A} = \begin{bmatrix} \exp(t) \sin(2\pi x) \sin(2\pi y) \\ \exp(t) \sin(2\pi y) \sin(2\pi z) \\ \exp(t) \sin(2\pi z) \end{bmatrix}$$

with

$$\mathbf{H}_e = \begin{bmatrix} -2\pi \exp(t) \sin(2\pi y) \cos(2\pi z) \\ 0 \\ -2\pi \exp(t) \sin(2\pi x) \cos(2\pi y) \end{bmatrix}.$$

We also set the terminate time $T = 1.0$ in this example.

A uniform tetrahedral mesh with $M + 1$ vertices in each direction of the cube is used in our computation, where $h = \frac{\sqrt{3}}{M}$. We solve the system by the Galerkin-mixed FEM scheme (2.10)-(2.12) with $(\mathcal{V}_h^r, \mathbf{Q}_h^{r+1} \times \mathbf{U}_h^r)$ for $r = 0, 1$, respectively. Here $\boldsymbol{\sigma} = \operatorname{curl} \mathbf{A}$ is a three dimensional vector function and correspondingly \mathbf{Q}_h^{r+1} is the $(r+1)$ -th order first type Nédélec element space. To confirm our error estimates in the L^2 norm, we choose $\tau = \left(\frac{1}{M}\right)^{r+1}$ for $(\mathcal{V}_h^r, \mathbf{Q}_h^{r+1} \times \mathbf{U}_h^r)$. We present in Table 4 the L^2 -norm errors of ψ , \mathbf{A} , $\boldsymbol{\sigma}$. We can see clearly that the L^2 norm errors are in the order of $O(h^{r+1})$, $r = 0, 1$, which confirm our error analysis in three dimensional space.

Table 4: L^2 norm errors of ψ , \mathbf{A} and $\boldsymbol{\sigma}$ on the unit cube (Example 5.3).

$(\mathcal{V}_h^1, \mathbf{Q}_h^1 \times \mathbf{U}_h^0)$	$\tau = \frac{1}{M}$	$\ \psi_h^N - \psi(\cdot, t_N)\ _{L^2}$	$\ \mathbf{A}_h^N - \mathbf{A}(\cdot, t_N)\ _{L^2}$	$\ \boldsymbol{\sigma}_h^N - \boldsymbol{\sigma}(\cdot, t_N)\ _{L^2}$
$M = 8$		2.0951e-01	7.0869e-01	3.9600e+00
$M = 16$		8.3881e-02	3.3623e-01	1.9502e+00
$M = 32$		3.7858e-02	1.6561e-01	9.7032e-01
order		1.234	1.049	1.015
$(\mathcal{V}_h^1, \mathbf{Q}_h^2 \times \mathbf{U}_h^1)$	$\tau = \frac{1}{M^2}$	$\ \psi_h^N - \psi(\cdot, t_N)\ _{L^2}$	$\ \mathbf{A}_h^N - \mathbf{A}(\cdot, t_N)\ _{L^2}$	$\ \boldsymbol{\sigma}_h^N - \boldsymbol{\sigma}(\cdot, t_N)\ _{L^2}$
$M = 4$		4.2803e-01	3.3717e-01	1.6782e+00
$M = 8$		1.0461e-01	8.9300e-02	4.4795e-01
$M = 16$		2.5907e-02	2.2832e-02	1.1670e-01
order		2.023	1.942	1.923

6 Conclusions

We analyzed a linearized backward Euler Galerkin-mixed FEM for the time-dependent Ginzburg–Landau equations in both two and three dimensional spaces. We have established unconditionally optimal error estimates for the three dimensional model, while analysis presented in this paper can be extended to many other cases, such as the two dimensional problem and Crank–Nicolson scheme. The method can solve for the induced magnetic field $\mathbf{curl} \mathbf{A}$ ($\mathbf{curl} \mathbf{A}$ in two dimensional space) accurately without corner singularities and the method is particularly suitable for nonconvex domains and domains with complex geometries. Numerical experiments presented in this paper show the efficiency of the method and confirm our theoretical analysis. Large scale parallel computations and adaptive local refinement or moving mesh strategy will be conducted in our future work.

Acknowledgment

The first author would like to thank Professor Douglas Arnold for useful discussions on mixed methods for vector Poisson equations.

References

- [1] A. Alonso and A. Valli, An optimal domain decomposition preconditioner for low-frequency time-harmonic Maxwell equations. *Math. Comput.*, 68(1999), pp 607–631.
- [2] T. Alstrom, M. Sorensen, N. Pedersen and S. Madsen, Magnetic flux lines in complex geometry type-II superconductors studied by the time dependent Ginzburg–Landau equation, *Acta Appl. Math.*, 115(2011), pp. 63–74.
- [3] C. Amrouche, C. Bernardi, M. Dauge and V. Girault, Vector potentials in three-dimensional non-smooth domains. *Math. Methods Appl. Sci.*, 21(1998), pp. 823–864.
- [4] D. Arnold, R. Falk and R. Winther, Finite element exterior calculus, homological techniques, and applications, *Acta Numer.*, 15(2006), pp. 1–155.
- [5] D. Arnold, R. Falk and R. Winther, Finite element exterior calculus: from Hodge theory to numerical stability, *Bull. Amer. Math. Soc. (N.S.)*, 47(2010), pp. 281–354.
- [6] J. Bergh and J. Lofstrom, *Interpolation spaces: An introduction*, Springer–Verlag, Berlin–New York, 1976.
- [7] D. Braess, *Finite Elements: Theory, Fast Solvers, and Applications in Elasticity Theory*, 3rd ed., Cambridge University Press, Cambridge, UK, 2007.
- [8] S. Brenner and L. Scott, *The Mathematical Theory of Finite Element Methods*, Springer, New York, 2002.
- [9] F. Brezzi and M. Fortin, *Mixed and Hybrid Finite Element Methods*, Springer, New York, 1991.
- [10] S. Chapman, S. Howison and J. Ockendon, Macroscopic models for superconductivity, *SIAM Rev.*, 34(1992), pp. 529–560.

- [11] P. Chatzipantelidis, R.D. Lazarov, V. Thomée and L.B. Wahlbin, Parabolic finite element equations in nonconvex polygonal domains, *BIT Numer. Math.*, 46(2006), pp. S113–S143.
- [12] Z. Chen, Mixed finite element methods for a dynamical Ginzburg–Landau model in superconductivity, *Numer. Math.*, 76(1997), pp. 323–353.
- [13] Z. Chen, K. Hoffmann, Numerical studies of a non-stationary Ginzburg–Landau model for superconductivity, *Adv. Math. Sci. Appl.*, 5(1995), pp. 363–389.
- [14] Z. Chen, K. Hoffmann and J. Liang, On a non-stationary Ginzburg–Landau superconductivity model, *Math. Methods Appl. Sci.*, 16(1993), pp. 855–875.
- [15] K. Chrysafinos and L.S. Hou, Error estimates for semidiscrete finite element approximations of linear and semilinear parabolic equations under minimal regularity assumptions, *SIAM J. Numer. Anal.*, 40(2002), pp. 282–306.
- [16] M. Dauge, *Elliptic Boundary Value Problems on Corner Domains*, Lecture Notes in Math.1341, Springer, Berlin, 1988.
- [17] M. Dauge, Singularities of corner problems and problems of corner singularities, *ESAIM Proc.*, 6 (1999), pp. 19–40.
- [18] Q. Du, Finite element methods for the time-dependent Ginzburg–Landau model of superconductivity, *Comput. Math. Appl.*, 27(1994), pp. 1–17.
- [19] Q. Du, Numerical approximations of the Ginzburg–Landau models for superconductivity, *J. Math. Phys.*, 46(2005), pp. 095–109.
- [20] Q. Du, M. Gunzburger and J. Peterson, Analysis and approximation of the Ginzburg–Landau model of superconductivity, *SIAM Rev.*, 34(1992), pp. 54–81.
- [21] E. Feireisl and P. Takac, Long-time stabilization of solutions to the Ginzburg–Landau equations of superconductivity, *Monatsh. Math.*, 133(2001), pp. 197–221.
- [22] H. Gao and W. Sun. An efficient fully linearized semi-implicit Galerkin-mixed FEM for the dynamical Ginzburg–Landau equations of superconductivity. *J. Comput. Phys.*, 294(2015), 329–345.
- [23] H. Gao, B. Li and W. Sun, Optimal error estimates of linearized Crank–Nicolson Galerkin FEMs for the time-dependent Ginzburg–Landau equations in superconductivity, *SIAM J. Numer. Anal.*, 52(2014), 1183–1202.
- [24] G. Gatica, *A Simple Introduction to the Mixed Finite Element Method. Theory and Applications*, Springer Briefs in Mathematics. Springer, New York, 2014.
- [25] V. Girault and P. Raviart, *Finite Element Methods for Navier–Stokes Equations*, Springer–Verlag, Berlin, 1986.
- [26] L. Gor’kov and G. Eliashberg, Generalization of the Ginzburg–Landau equations for non-stationary problems in the case of alloys with paramagnetic impurities, *Soviet Phys.-JETP*, 27(1968), pp. 328–334.
- [27] W. Gropp, H. Kaper, G. Leaf, D. Levine, M. Palumbo and V. Vinokur, Numerical simulation of vortex dynamics in type-II superconductors, *J. Comput. Phys.*, 123(1996), pp. 254–266.

- [28] D. Gunter, H. Kaper and G. Leaf, Implicit integration of the time-dependent Ginzburg–Landau equations of superconductivity, *SIAM J. Sci. Comput.*, 23(2002), pp. 1943–1958.
- [29] C. Levermore and M. Oliver, *The complex Ginzburg–Landau equation as a model problem*, Lectures Appl. Math., 31(1996), pp. 141–190.
- [30] B. Li and C. Yang, Global well-posedness of the time-dependent Ginzburg–Landau superconductivity model in curved polyhedra, *arXiv:1411.4235*.
- [31] B. Li and Z. Zhang, Mathematical and numerical analysis of time-dependent Ginzburg–Landau equations in nonconvex polygons based on Hodge decomposition, *arXiv:1410.3547v2*.
- [32] B. Li and Z. Zhang, A new approach for numerical simulation of the time-dependent Ginzburg–Landau equations, *arXiv:1410.3746v2*.
- [33] A. Logg, K. Mardal and G. Wells (Eds.), *Automated Solution of Differential Equations by the Finite Element Method*, Springer, Berlin, 2012, [DOI:10.1007/978-3-642-23099-8].
- [34] M. Mu, A linearized Crank–Nicolson–Galerkin method for the Ginzburg–Landau model, *SIAM J. Sci. Comput.*, 18(1997), pp. 1028–1039.
- [35] M. Mu and Y. Huang, An alternating Crank–Nicolson method for decoupling the Ginzburg–Landau equations, *SIAM J. Numer. Anal.*, 35(1998), pp. 1740–1761.
- [36] L. Nirenberg, An extended interpolation inequality, *Ann. Scuola Norm. Sup. Pisa (3)*, 20(1966), pp. 733–737.
- [37] W. Richardson, A. Pardhanani, G. Carey and A. Ardelea, Numerical effects in the simulation of Ginzburg–Landau models for superconductivity, *Int. J. Numer. Meth. Engng.*, 59(2004), 1251–1272.
- [38] A. Rodriguez–Bernal, B. Wang and R. Willie, Asymptotic behavior of the time-dependent Ginzburg–Landau equations of superconductivity, *Math. Methods Appl. Sci.*, 22(1999), pp. 1647–1669.
- [39] Q. Tang and S. Wang, Time dependent Ginzburg–Landau equations of superconductivity, *Physica D*, 88(1995), pp. 139–166.
- [40] V. Thomee, *Galerkin Finite Element Methods for Parabolic Problems*, Springer–Verlag, Berlin, 2006.
- [41] T. Winiecki and C. Adams, A fast semi-implicit finite difference method for the TDGL equation, *J. Comput. Phys.*, 179(2002), pp. 127–139.

Appendix

With all the notations in section 2, for any given $e_{\mathbf{A}}^n \in \mathring{\mathbf{U}}_h^r$, if there exists a $e_{\boldsymbol{\sigma}}^n \in \mathring{\mathbf{Q}}_h^{r+1}$ such that

$$(e_{\boldsymbol{\sigma}}^n, \boldsymbol{\chi}_h) - (\mathbf{curl} \boldsymbol{\chi}_h, e_{\mathbf{A}}^n) = 0, \quad \forall \boldsymbol{\chi}_h \in \mathring{\mathbf{Q}}_h^{r+1}, \quad (6.1)$$

then the following discrete Sobolev embedding inequality holds

$$\|e_{\mathbf{A}}^n\|_{L^3} \leq C (\|e_{\boldsymbol{\sigma}}^n\|_{L^2} + \|\operatorname{div} e_{\mathbf{A}}^n\|_{L^2}). \quad (6.2)$$

Proof:

From the Hodge decomposition [4, 5], the following exact sequence holds:

$$\begin{array}{ccccccc} \mathring{\mathbf{H}}(\mathbf{curl}) & \xrightarrow{\mathbf{curl}} & \mathring{\mathbf{H}}(\operatorname{div}) & \xrightarrow{\operatorname{div}} & L_0^2 & & \\ \downarrow & & \downarrow & & \downarrow & & \\ \mathring{\mathbf{Q}}_h^{r+1} & \xrightarrow{\mathbf{curl}} & \mathring{\mathbf{U}}_h^r & \xrightarrow{\operatorname{div}} & \mathring{\mathbf{S}}_h^r & & \end{array}$$

where $L_0^2 = \{v \in L^2 \mid (v, 1) = 0\}$ and $\mathring{\mathbf{S}}_h^r = \mathbf{S}_h^r \cap L_0^2$ with

$$\mathbf{S}_h^r := \{v \in L^2(\Omega) \mid \forall \Omega_K \in \mathcal{T}_h, v|_{\Omega_K} \text{ is a polynomial of degree } r\}.$$

Then, we have

$$\mathring{\mathbf{U}}_h^r = \mathbf{curl} \mathring{\mathbf{Q}}_h^{r+1} \oplus \mathbf{grad}_h \mathring{\mathbf{S}}_h^r, \quad (6.3)$$

where \oplus denotes the direct sum and the linear operator $\mathbf{grad}_h : \mathring{\mathbf{S}}_h^r \rightarrow \mathring{\mathbf{U}}_h^r$ is defined as: for any given $s_h \in \mathring{\mathbf{S}}_h^r$, find $\mathbf{grad}_h s_h \in \mathring{\mathbf{U}}_h^r$ such that

$$(\mathbf{grad}_h s_h, \mathbf{v}_h) = -(s_h, \operatorname{div} \mathbf{v}_h), \quad \forall \mathbf{v}_h \in \mathring{\mathbf{U}}_h^r. \quad (6.4)$$

Therefore, for any given $e_{\mathbf{A}}^n \in \mathring{\mathbf{U}}_h^r$, there exist $\boldsymbol{\theta}_h \in \mathring{\mathbf{Q}}_h^{r+1}$ and $s_h \in \mathring{\mathbf{S}}_h^r$ such that

$$e_{\mathbf{A}}^n = \mathbf{curl} \boldsymbol{\theta}_h \oplus \mathbf{grad}_h s_h \quad (6.5)$$

To prove (6.2), we only need to show

$$\|\mathbf{grad}_h s_h\|_{L^3} + \|\mathbf{curl} \boldsymbol{\theta}_h\|_{L^3} \leq C (\|e_{\boldsymbol{\sigma}}^n\|_{L^2} + \|\operatorname{div} e_{\mathbf{A}}^n\|_{L^2}).$$

We first estimate $\mathbf{grad}_h s_h$. Indeed, $\mathbf{grad}_h s_h$ can be viewed as the mixed FEM solution to the following Poisson equation with pure Neumann boundary condition

$$\begin{cases} -\Delta u = \operatorname{div} e_{\mathbf{A}}^n & \text{in } \Omega \\ \nabla u \cdot \mathbf{n} = 0 & \text{on } \partial\Omega \end{cases} \quad (6.6)$$

It should be noted that the regularity for (6.6) depends upon the the domain Ω , see [16, 17]. For a general polyhedron in three dimensional space, we have the following shift theorem

$$\|u\|_{H^{3/2+\alpha}} \leq C \|\operatorname{div} e_{\mathbf{A}}^n\|_{H^{-1/2+\alpha}}, \quad (6.7)$$

where $\alpha > 0$ depends only upon the geometry of the polyhedron. The classical mixed FEM for solving (6.6) is to find $(\mathbf{q}_h, u_h) \in (\mathring{\mathbf{U}}_h^r, \mathring{\mathbf{S}}_h^r)$ such that

$$\begin{cases} (\mathbf{q}_h, \mathbf{v}_h) + (u_h, \operatorname{div} \mathbf{v}_h) = 0 & \forall \mathbf{v}_h \in \mathring{\mathbf{U}}_h^r, \\ -(\operatorname{div} \mathbf{q}_h, \mu_h) = (\operatorname{div} e_{\mathbf{A}}^n, \mu_h) & \forall \mu_h \in \mathring{\mathbf{S}}_h^r. \end{cases}$$

From (6.4) and (6.5), one can verify that $\mathbf{grad}_h s_h = \mathbf{q}_h$. By using an inverse inequality and the classical error estimates of mixed methods for elliptic equation [7, 9], we can deduce that

$$\begin{aligned}
\|\mathbf{grad}_h s_h\|_{L^3} &\leq \|\mathbf{grad}_h s_h - \pi_h \nabla u\|_{L^3} + \|\pi_h \nabla u\|_{L^3} \\
&\leq Ch^{-\frac{1}{2}} \|\mathbf{grad}_h s_h - \pi_h \nabla u\|_{L^2} + \|u\|_{H^{3/2+\alpha}} \\
&\leq Ch^{-\frac{1}{2}} (\|\mathbf{grad}_h s_h - \nabla u\|_{L^2} + \|\pi_h \nabla u - \nabla u\|_{L^2}) + C \|\operatorname{div} e_{\mathbf{A}}^n\|_{L^2} \\
&\leq Ch^{-\frac{1}{2}} h^{\frac{1}{2}+\alpha} \|\nabla u\|_{H^{1/2+\alpha}} + C \|\operatorname{div} e_{\mathbf{A}}^n\|_{L^2} \\
&\leq C \|\operatorname{div} e_{\mathbf{A}}^n\|_{L^2},
\end{aligned} \tag{6.8}$$

where π_h is the projection operator defined in (2.9).

Now we turn to estimate $\mathbf{curl} \boldsymbol{\theta}_h$. From the discrete Hodge decomposition (6.5), we have

$$(\mathbf{curl} \boldsymbol{\theta}_h, \mathbf{curl} \boldsymbol{\chi}_h) = (e_{\mathbf{A}}^n, \mathbf{curl} \boldsymbol{\chi}_h) = (e_{\boldsymbol{\sigma}}^n, \boldsymbol{\chi}_h) \quad \text{for any } \boldsymbol{\chi}_h \in \mathring{\mathbf{Q}}_h^{r+1}.$$

A key observation is that $\boldsymbol{\theta}_h$ can be viewed as the mixed finite element solution to the vector Poisson equation

$$\begin{cases} \mathbf{curl} \mathbf{curl} \mathbf{u} - \nabla \operatorname{div} \mathbf{u} = e_{\boldsymbol{\sigma}}^n & \text{in } \Omega \\ \mathbf{u} \times \mathbf{n} = \mathbf{0}, \operatorname{div} \mathbf{u} = 0, & \text{on } \partial\Omega \end{cases} \tag{6.9}$$

which is to find $(\phi_h, \mathbf{u}_h) \in \mathring{V}_h^r \times \mathring{\mathbf{Q}}_h^{r+1}$, where \mathring{V}_h^r denote the r -th Lagrange element space with zero trace, such that

$$\begin{cases} -(\phi_h, \zeta_h) + (\mathbf{u}_h, \nabla \zeta_h) = 0, & \text{for any } \zeta_h \in \mathring{V}_h^r. \\ (\nabla \phi_h, \boldsymbol{\chi}_h) + (\mathbf{curl} \mathbf{u}_h, \mathbf{curl} \boldsymbol{\chi}_h) = (e_{\boldsymbol{\sigma}}^n, \boldsymbol{\chi}_h), & \text{for any } \boldsymbol{\chi}_h \in \mathring{\mathbf{Q}}_h^{r+1}. \end{cases} \tag{6.10}$$

Since $\boldsymbol{\theta}_h = \mathbf{u}_h$, from the standard error estimate [4, 5], we have

$$\begin{aligned}
&\|\operatorname{div} \mathbf{u} - \phi_h\|_{L^2} + \|\mathbf{u} - \boldsymbol{\theta}_h\|_{\mathbf{H}(\mathbf{curl})} \\
&\leq C \left(\inf_{\zeta_h \in \mathring{V}_h^r} \|\operatorname{div} \mathbf{u} - \zeta_h\|_{L^2} + \inf_{\boldsymbol{\chi}_h \in \mathring{\mathbf{U}}_h^r} \|\mathbf{u} - \boldsymbol{\chi}_h\|_{\mathbf{H}(\mathbf{curl})} \right)
\end{aligned} \tag{6.11}$$

Thus, with the projection operator π_h in (2.9), we can derive the following estimates

$$\begin{aligned}
\|\mathbf{curl} \boldsymbol{\theta}_h\|_{L^3} &\leq \|\mathbf{curl} \boldsymbol{\theta}_h - \mathbf{curl} \pi_h \mathbf{u}\|_{L^3} + \|\mathbf{curl} \pi_h \mathbf{u}\|_{L^3} \\
&\leq Ch^{-\frac{1}{2}} \|\mathbf{curl} \boldsymbol{\theta}_h - \mathbf{curl} \mathbf{u}\|_{L^2} + Ch^{-\frac{1}{2}} \|\mathbf{curl} \pi_h \mathbf{u} - \mathbf{curl} \mathbf{u}\|_{L^2} + \|e_{\boldsymbol{\sigma}}^n\|_{L^2} \\
&\leq Ch^{-\frac{1}{2}} \|\mathbf{curl} \pi_h \mathbf{u} - \mathbf{curl} \mathbf{u}\|_{L^2} + \|e_{\boldsymbol{\sigma}}^n\|_{L^2} \\
&\leq Ch^{-\frac{1}{2}} h^{\frac{1}{2}+\alpha} (\|\mathbf{curl} \mathbf{u}\|_{H^{1/2+\alpha}} + \|\operatorname{div} \mathbf{u}\|_{H^{1/2+\alpha}}) + \|e_{\boldsymbol{\sigma}}^n\|_{L^2} \\
&\leq C \|e_{\boldsymbol{\sigma}}^n\|_{L^2},
\end{aligned} \tag{6.12}$$

where we have used an inverse inequality and noted that in (6.10)

$$\|\mathbf{curl} \mathbf{u}\|_{H^{1/2+\alpha}} + \|\operatorname{div} \mathbf{u}\|_{H^{1/2+\alpha}} \leq C \|e_{\boldsymbol{\sigma}}^n\|_{L^2} \tag{6.13}$$

for a certain $\alpha > 0$, see [1, 3].

The embedding inequality (6.2) is proved by combining (6.8) and (6.12). \blacksquare

Remark 6.1 *The discrete embedding inequality (6.2) is enough in the error analysis of the Galerkin-mixed FEM for the TDGL equations. However, if the polyhedron Ω is convex we can derive a stronger discrete embedding inequality*

$$\|e_{\mathbf{A}}^n\|_{L^6} \leq C (\|e_{\boldsymbol{\sigma}}^n\|_{L^2} + \|\operatorname{div} e_{\mathbf{A}}^n\|_{L^2}) . \quad (6.14)$$

On a convex domain, we have $\alpha > \frac{1}{2}$ in (6.7) for the shift theorem. And then, we have

$$\begin{aligned} \|\mathbf{grad}_h s_h\|_{L^6} &\leq \|\mathbf{grad}_h s_h - \pi_h \nabla u\|_{L^6} + \|\pi_h \nabla u\|_{L^6} \\ &\leq Ch^{-1} \|\mathbf{grad}_h s_h - \pi_h \nabla u\|_{L^2} + \|u\|_{H^2} \\ &\leq C \|\operatorname{div} e_{\mathbf{A}}^n\|_{L^2} . \end{aligned} \quad (6.15)$$

Moreover, for a convex domain Ω , the embedding inequality (6.13) can be re-written by

$$\|\mathbf{curl} \mathbf{u}\|_{H^1} + \|\operatorname{div} \mathbf{u}\|_{H^1} \leq C \|e_{\boldsymbol{\sigma}}^n\|_{L^2}, \quad (6.16)$$

which implies

$$\|\mathbf{curl} \boldsymbol{\theta}_h\|_{L^6} \leq C \|e_{\boldsymbol{\sigma}}^n\|_{L^2}. \quad (6.17)$$

Remark 6.2 *The discrete Hodge decomposition (6.3) is only valid for simply-connected domain. If the domain Ω is multi-connected, we have*

$$\mathring{\mathbf{U}}_h^r = \mathbf{curl} \mathring{\mathbf{Q}}_h^{r+1} \oplus \mathbf{grad}_h \mathring{\mathbf{S}}_h^r \oplus \mathbf{Har}_h^r, \quad (6.18)$$

where $\mathbf{Har}_h^r := \{\mathbf{v}_h \in \mathring{\mathbf{U}}_h^r \mid \operatorname{div} \mathbf{v}_h = 0, (\mathbf{v}_h, \mathbf{curl} \boldsymbol{\chi}_h) = 0, \forall \boldsymbol{\chi}_h \in \mathring{\mathbf{Q}}_h^{r+1}\}$ stands for the harmonic part of $\mathring{\mathbf{U}}_h^r$. In this case,

$$e_{\mathbf{A}}^n = \mathbf{curl} \boldsymbol{\theta}_h \oplus \mathbf{grad}_h s_h \oplus \mathbf{v}_h,$$

where $\mathbf{v}_h \in \mathbf{Har}_h^r$. we can prove the following inequality via a similar analysis

$$\|\mathbf{v}_h\|_{L^3} \leq C (\|e_{\boldsymbol{\sigma}}^n\|_{L^2} + \|\operatorname{div} e_{\mathbf{A}}^n\|_{L^2}) .$$